December 2004 • NREL/SR-520-37212

Subcontractor Report

Development of an In-line Minority-Carrier Lifetime Monitoring Tool for Process Control during Fabrication of Crystalline Silicon Solar Cells

Final Technical Report
2 August 2002–15 November 2004

R.A. Sinton
Sinton Consulting, Inc.
Boulder, Colorado

National Renewable Energy Laboratory
1617 Cole Boulevard, Golden, Colorado 80401-3393
303-275-3000 • www.nrel.gov

Operated for the U.S. Department of Energy
Office of Energy Efficiency and Renewable Energy
by Midwest Research Institute • Battelle

Contract No. DE-AC36-99-GO10337

December 2004 • NREL/SR-520-37212

Development of an In-line Minority-Carrier Lifetime Monitoring Tool for Process Control during Fabrication of Crystalline Silicon Solar Cells

Final Technical Report
2 August 2002–15 November 2004

R.A. Sinton
Sinton Consulting, Inc.
Boulder, Colorado

NREL Technical Monitors: D. Mooney and K. Brown

Prepared under Subcontract No. ZDO-2-30628-08

National Renewable Energy Laboratory
1617 Cole Boulevard, Golden, Colorado 80401-3393
303-275-3000 • www.nrel.gov

Operated for the U.S. Department of Energy
Office of Energy Efficiency and Renewable Energy
by Midwest Research Institute • Battelle

Contract No. DE-AC36-99-GO10337

Table of Contents

List of Figures

Abstract

As the production volumes of crystalline silicon manufacturing lines have grown in recent years, the demand for improved process control and process monitoring in manufacturing has increased.

Under the PV Manufacturing R&D subcontract "Development of an In-Line, Minority-Carrier Lifetime Monitoring Tool for Process Control During Fabrication of Crystalline Silicon Solar Cells", Sinton Consulting developed prototypes for several new instruments for use in the manufacture of silicon solar cells. Four instruments have now been extensively tested through collaborations with industry. A major accomplishment was the integration of discrete "breadboard" components into instruments optimized for each production application. For each instrument and application, substantial R&D work was required to develop the device physics and analysis in addition to the hardware. Of particular importance was the development of methodologies to calibrate lifetime measurements for use on industrial samples, including the measurement of unpassivated wafers as they exist in the production line and the measurement of multicrystalline bricks to determine lifetime, trapping, and iron concentration as a function of position. Although motivated to provide the development and documentation necessary for industrial applications of the instruments, these results have also been presented in 12 publications at technical conferences as contributions to silicon photovoltaics R&D.

Acknowledgements: Special thanks to Victoria Nosal, Ed Witt, Christie Johnson, Carolyn Lopez, David Mooney, and Katie Brown for guiding us through this DOE subcontract. Much of the technical work in this report was made possible by the contributions of Tanaya Mankad, Stuart Bowden, and Peter Jackson. Industrial and academic collaborators included Nicolas Enjalbert at Photowatt SA, Harsharn Tathgar at Scanwafer, Jeff Nickerson at Shell Solar, John Coleman at University of Northern Colorado, and Andres Cuevas at the Australian National University. Many others have also made contributions to this work.

Introduction

The objective of this subcontract over its two-phase, two year duration was to design and develop improvements to the existing Sinton Consulting R&D minority-carrier lifetime testers. The improvements enable the possibilities for performing various in-line diagnostics on crystalline silicon wafers and cells for solar cell manufacturing lines. This facilitates manufacturing optimization and improved process control.

The scope of work for Phase I was to prototype industrial applications for the improved instruments. A small-sample-head version of the instrument was to be designed and developed in this effort. This new instrument was to be complemented by detailed application notes detailing the productive use of minority-carrier lifetime measurements for process optimization and routine process control.

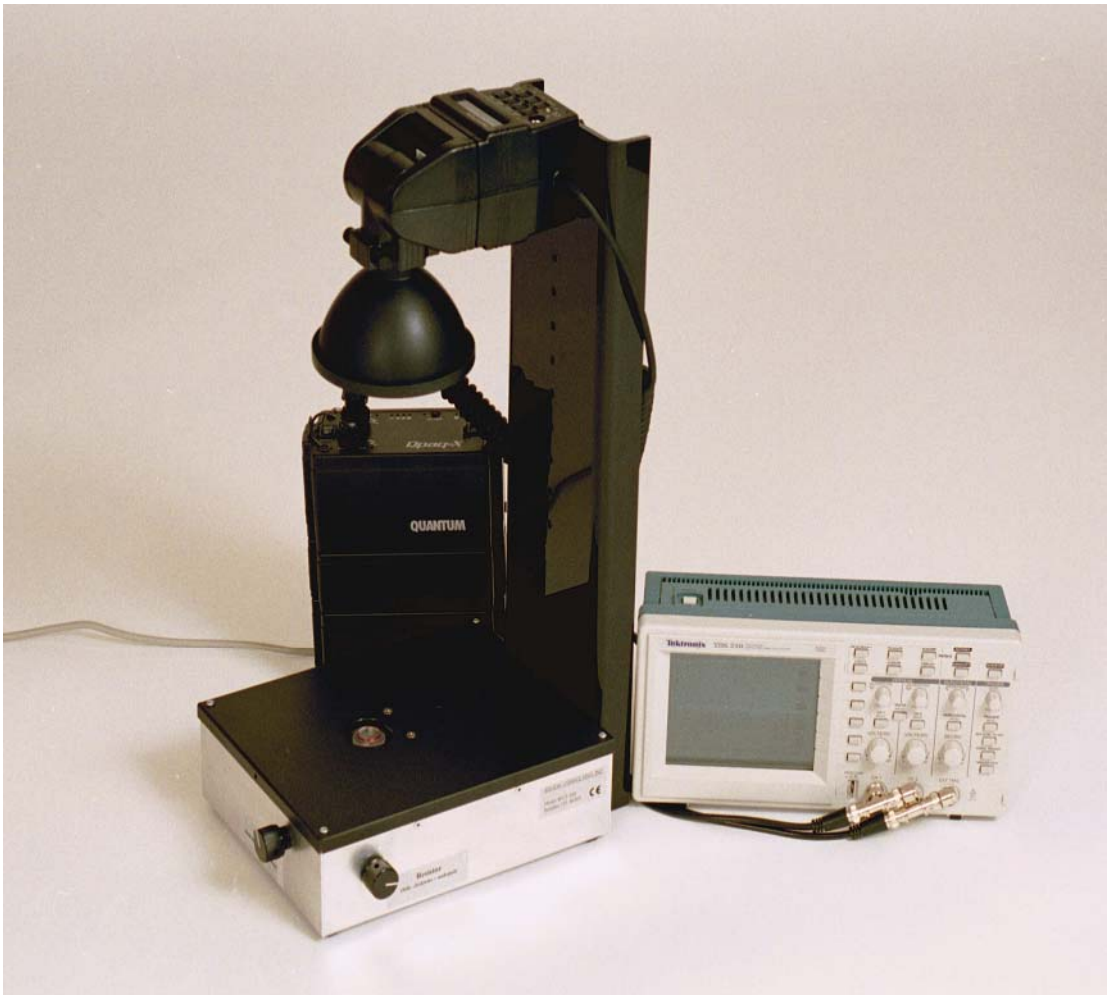

Fig. 1. The starting point for this subcontract. Over 120 Sinton Consulting lifetime testers are used worldwide. This instrument is primarily applied to taking detailed measurements on carefully-prepared single wafers in an R&D setting. Industrial applications and industrial versions of this measurement technique will be discussed in this final subcontract report.

In Phase 2, the results from the first year to were applied to design new instruments for industrial applications. These instruments were then characterized and documented.

We report here on four new instruments, each optimized for a specific application as demanded by industrial customers. The documentation for these instruments was very technical and involved considerable R&D. Applications were developed that applied the latest in R&D on industrial silicon materials. By investigating the compromises that would be necessary to measure industrial material directly without the sample preparation that is commonly done for good research, we were able to develop several very innovative applications that can now be done directly in the production line for process control.

These applications include the measurement of long-lifetime photovoltaic silicon directly in the bricks or boules without surface preparation, the determination of bulk lifetime in multicrystalline wafers by measurement on unpassivated as-cut wafers, and the mapping of lifetime, Fe concentration, and trapping behavior in multicrystalline silicon bricks at rates that would permit the measurement of every brick in the production line. These new applications are expected to encourage industrial demand for the new tools.

During the engineering of the new industrial tools, industrial site visits were used to get feedback and test the equipment against the requirements of industry. Several technical papers resulted from these industrial collaborations. These publications will help to establish the technical credibility of the new instruments and measurement methodologies. Much of the work described in this final report is drawn from these publications.

Phase I. 12 months starting August 2002

Task 1. Prototype Industrial Applications Using Existing or Modified Instruments

The R&D minority-carrier lifetime tester(15) from Sinton Consulting required considerable skill and understanding for successful measurements. An important goal of Task 1 in this subcontract was to refine the instrument, the measurement procedures, and the software in order to eliminate the necessity of operator discretion and intervention for measuring individual wafers.

This goal was largely achieved by working with the original R&D instrument, the WCT-100, and optimizing the procedures, software analysis and the hardware. In the new procedure, the measurement is referenced to an undoped wafer instead of the dark conductance of the wafer under test. In this way, the instrument can be "zeroed" once for an undoped wafer and then left unattended. Each measurement will then be taken referenced to this undoped wafer. By doing this, the full non-linear calibration curves for the instrument output response vs. conductance could be implemented. These calibration curves are also referenced to an undoped wafer. This improved the accuracy of the instrument as well as the usability. Some hardware improvements were incorporated in order to minimize the long-term instrument drift from this initial calibration.

In order not to lose sensitivity by referencing a conductance far from the conductance of the wafer under test, auto-scaling of the gain and voltage offset was implemented into the hardware and software. This improvement removed the necessity for the user to be an oscilloscope expert. Now, results from a novice user are rather indistinguishable from the results that an experienced scientist would obtain.

Data published from the R&D instrument generally uses the full injection-level lifetime curve in order to draw conclusions about the data. At the start of this project, it was thought that analysis simplifications would be required in order to achieve the high-speed measurements that would enable in-line wafer testing or block scanning. One of the first accomplishments of this work was to implement a fast data acquisition card to replace the digital oscilloscope previously used. This, in combination with better database implementation, allowed the complete R&D analysis to be so quick that these functions did not limit the rate at which data could be obtained, analyzed and logged. It was found that the inclusion of the full analysis allows the direct porting of methods used in the R&D labs to the industrial applications, without compromising the analysis flexibility or data quality. A new interface sits on top of the full data analysis in order to present the user with a limited spectrum of options completely specialized for the task at hand. In the background, the complete analysis is implemented and this reports back a simplified set of results to the user.

This results in a façade of a simple program and interface, while the results can have the same credibility as those that might be published from the R&D lab. An example of a simplified interface is presented under Task 2.

A demonstration of the implemented improvements is shown in Figure 1. One subtask of Task 1 was to demonstrate the Suns-V_{oc} technique(16) at high speed, suitable for automation. This technique allows the construction of a current-voltage curve as soon as the diffusion is formed on the wafer by simply probing the two polarity regions of the wafer. The open circuit voltage as a function of the illumination intensity is then measured and converted to a presentation analogous to the final solar cell I-V curve.

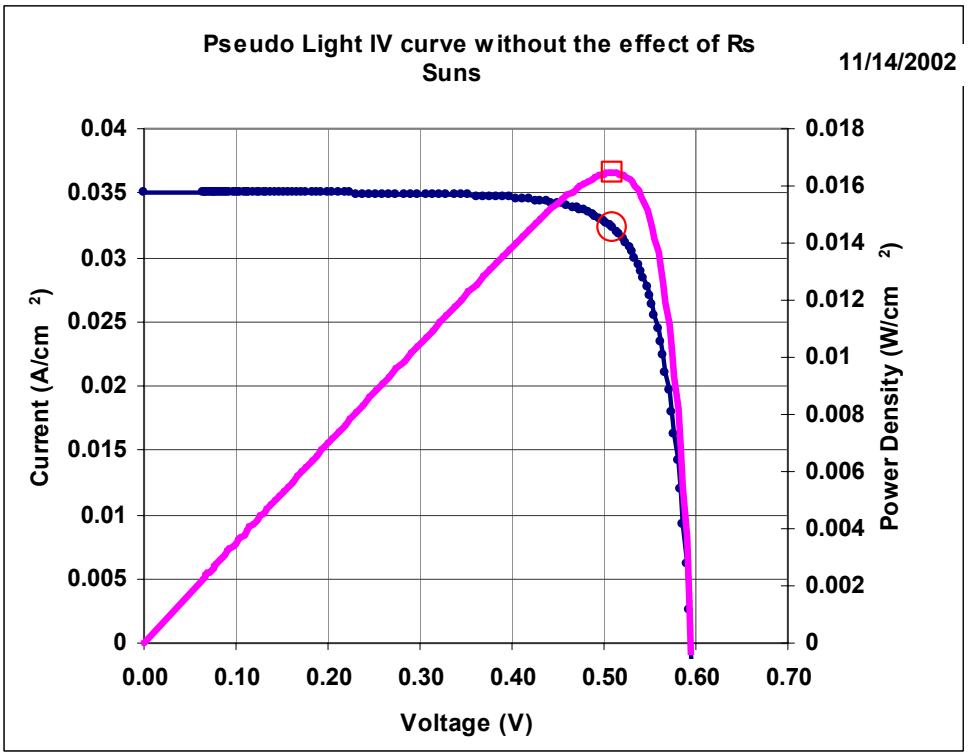

Fig. 2. The Pseudo-IV curve from a high-quality 100 cm^2 solar cell. This is the result that would be expected from a solar cell that had no series resistance.

It is most easily used after Al back-surface field formation, when the substrate is electrically accessible simply by placing the wafer on a conductive chuck. The resulting curve gives the upper bound possible for efficiency, since the data is taken under open-circuit conditions and involves no current flow. This illumination vs. open-circuit voltage technique was implemented using this new hardware and software interface. Fig. 2 and 3 show examples of data taken at a high rate, one wafer per two seconds.

This data in Figure 2 required that accurate voltage and illumination data be taken over two orders of magnitude (in illumination) within a fraction of a second. The fast data acquisition and analysis allows a large number of points to be taken at high resolution. The result has quite low noise. The longer term stability and standard deviation for a large number of measurements taken at high speed is shown in Fig. 3. For example, the measured "Pseudo fill factor" of this curve is 0.7906 +/- 0.0003, giving a standard deviation of 0.04% over these 3000 measurements taken in 100 minutes.

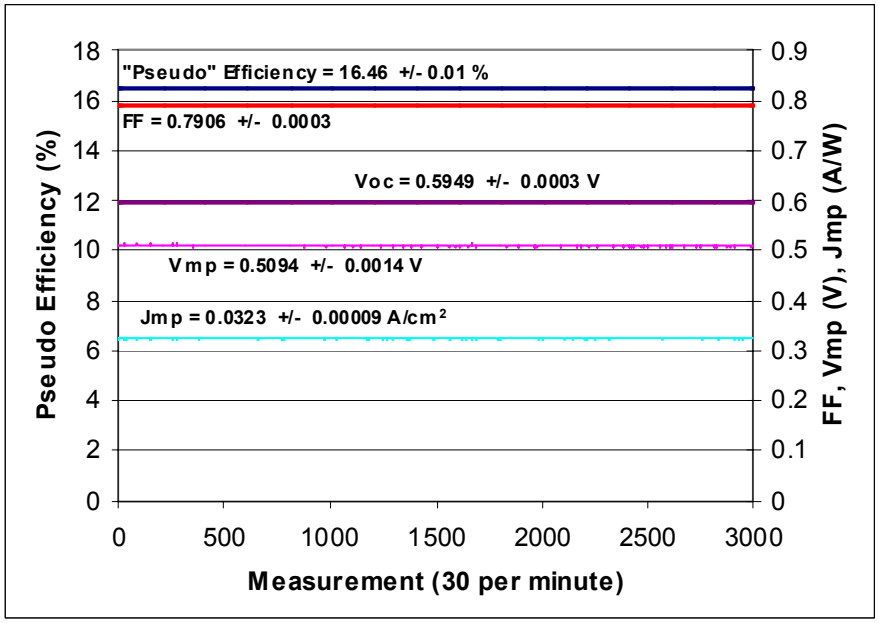

Fig. 3. A demonstration of the repeatability and speed of the measurement. 3000 measurements were taken on a single wafer at a rate of 30 per minute. With automation of the wafer handling, this could have been 3000 wafers.

Demonstration of the spectral response of the photoconductance was another subtask called out in Task 1. This was implemented on several instruments and used to optimize measurements on bare wafers and silicon blocks. This is reported under Task 2.

Task 2. Design, Engineer and Test a Small Sample Head Suitable for Use Inline

The intention of this task was to develop a small sample-head version of the lifetime tester with the flexibility to address applications for inline wafer testing and measurements on industrial multi-crystalline and CZ blocks or boules of silicon. This task was expected to result in a prototype design that could be used as the basis for an instrument for industrial early-adopters of lifetime testing.

In fact, it quickly became obvious that this task should be accelerated, in order to obtain proof of concepts for the instruments. The ideal proof of concept is one that gives a portfolio of data analysis results that can be sent around in order to focus a discussion with industry on near-term as well as long-term applications of the instrument to particular problems. Once this is done, industrial interest drives easy cooperation with significant industry involvement including sample exchanges, discussions, and on-site experiments. This helps to define the most relevant and useful designs and requirements for the instruments.

This strategy resulted in prototypes of four different lifetime-test instruments in this first year. Two of these have already been placed in industry, and are generating published as well as unpublished data that is contributing to further improvements in the instruments and measurement techniques. The following will briefly introduce these four instruments, as well as

a key result or two from each. These instruments are an ingot lifetime tester for use on CZ material prior to sawing(6), a block-test line-scanner for use on multicrystalline blocks prior to sawing(19), an FZ boule tester capable of characterizing the new generations of long-lifetime, low-cost FZ material to be used in low-cost 20% production silicon solar cells(22,25,29), and a small sample head suitable for integration into a production line as an in-line lifetime tester for each wafer at the start of the process(17) as well as at latter stages such as directly after the phosphorus diffusion(24).

A key enabling technology for these instruments was the design of a small, maneuverable instrument that could be placed on irregularly shaped samples (cylindrical, flat, etc.). Also, the light source was integrated into the instrument so that the illumination and the photoconductance sensing is from the same side of the sample. As shown in Figure 1, the previous R&D instrument had open-air illumination giving a uniform, large area illumination on a wafer and a reference cell. The photoconductance sensor was underneath the wafer on the opposite side from the illumination. In order to measure blocks, this had to be changed so that the portion of the block that would be illuminated on one side was also the portion where the sensor would monitor photoconductance. The reference cell was made to be internal to the instrument as well. This compact design forms the basis for all four instruments in this section. Each instrument and analysis is different for the four applications. However, many of the design parts are in common, simplifying the manufacture of instruments to serve these different applications.

An Instrument for Measuring the Lifetime on Solar CZ Silicon Ingots

This instrument was optimized to measure lifetime in the range of 1-100 microseconds on ingots that have no sample preparation. Ingots would simply be pulled from the existing processes and measured. This instrument is shown in Fig.s 4 and 5.

With the critical lifetime to be measured normally in the range of 10 μs, the Quasi-steady-state photoconductance (QSSPC) method gives much more robust results than the transient PCD method with this instrument(1). Infra-red light is used as the excitation source. This light is absorbed deep within the silicon. Much of the photogeneration is deeper than the diffusion length in this material. In this case, the measured lifetime becomes relatively indicative of the bulk lifetime, even for as-sawn or as-ground surfaces with very high surface recombination velocities.

The theory for QSSPC on blocks of silicon within the range of solar silicon has been investigated, with the results developed into an application note(26). Some of these results were presented at the 2003 PVSEC conference in Osaka as well(17).

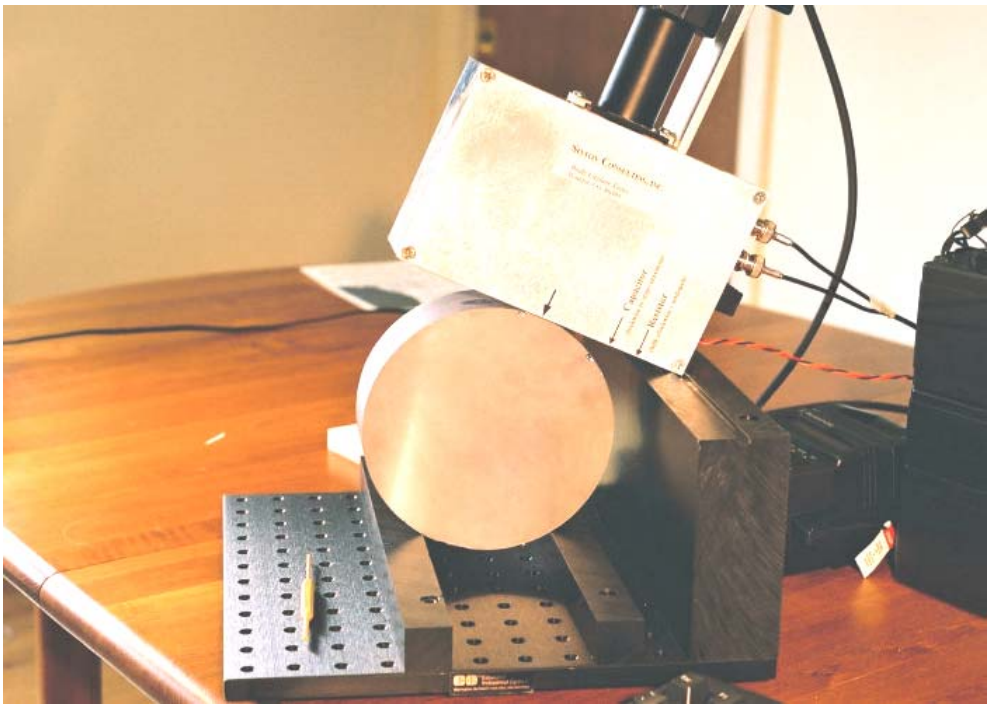

Fig. 4. A small sample head used in a configuration allowing the measurement of the lifetime in CZ silicon ingots. A section of an ingot is shown here.

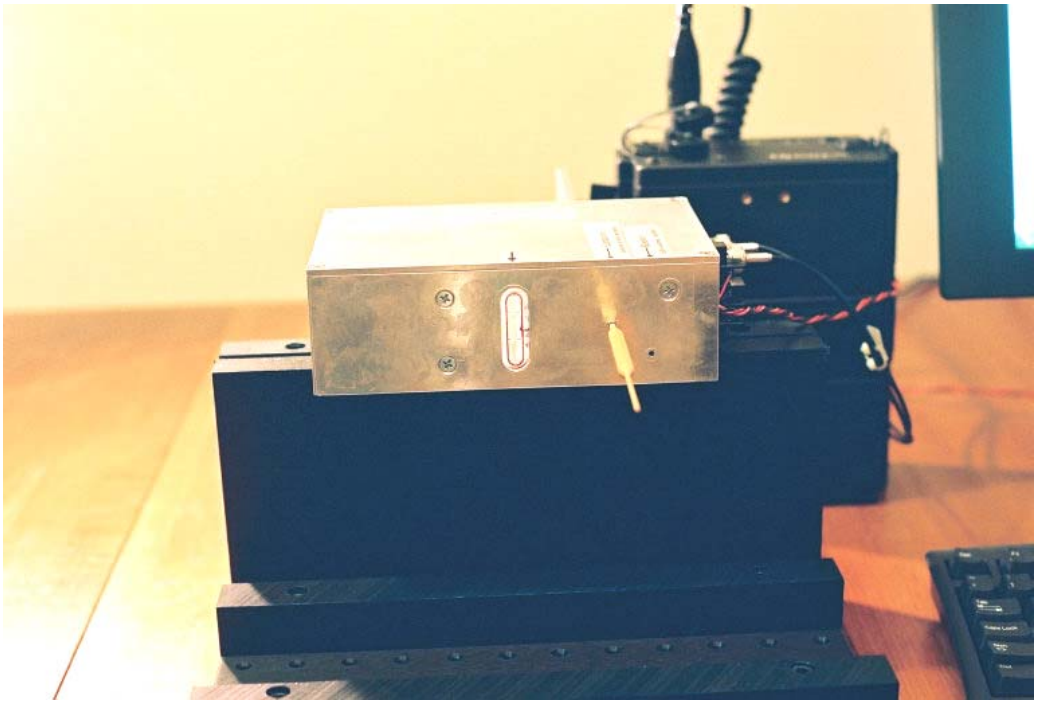

Fig. 5. The shape of the sensor is optimized for flexible measurements of blocks. The relatively large area gives a large photoconductance signal, and insures that the device physics of the analysis is primarily one-dimensional. The long slender shape of the sensor permits measurements on cylindrical shapes, since the sensor and illumination is nearly planar to the sensed portion of a cylindrical ingot when used in the geometry shown in Fig. 4.

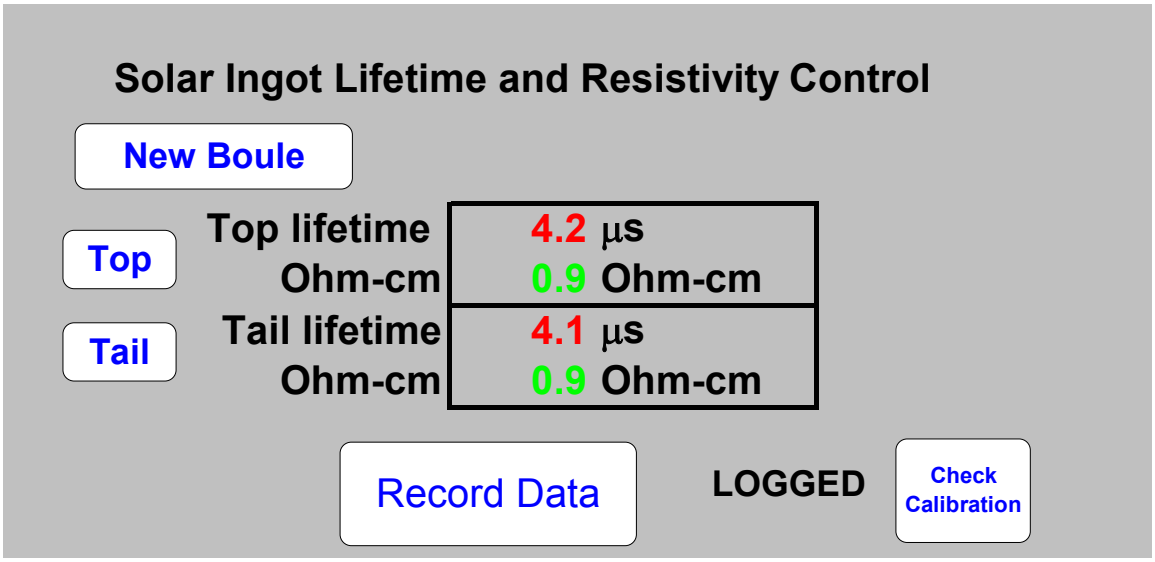

Figure 6. An example of a simplified interface. Although the device physics analysis is done with the same completeness as in the R&D instrument, a small subset of user input and analysis output is displayed on the user interface. This standardizes the measurement for a wide range of user types. To the user, the system is simple and the data is repeatable. The analysis results are color coded. Red results "fail", green results "pass".

Figure 6 shows an example of a simplified user interface suitable for industrial application. In this case, the user pushes a button, and a window pops up to accept the sample name. To measure the silicon, the operator places the instrument on the sample and pushes a button ("top" or "tail"). When finished, the data is logged to the database. Unseen by the operator, the QSSPC analysis is applied with a fixed interpretation previously set up by the engineer. This data analysis can specify the injection level to report the result, a bias light analysis to correct for trapping, and any of the other analysis techniques common to the QSSPC method. This system results in very uniform data results that are simple to obtain and are rather operator independent since there is little discretion in the measurement or analysis at the operator level.

A Multi-Crystalline Block Scanner

Figure 7 shows an instrument for measuring the lifetime of a multicrystalline block. This instrument performs a line scan down the length of the block, with high resolution (2 mm). This data can be used to determine the good region of the block from which to saw wafers. The data will also be used to optimize the growth process. Knowing the quality and spatial uniformity of the silicon directly after growth (and cutting into blocks) will allow short-loop optimization of the growth process. This information will be especially valuable since it can be done directly after growth, and it is independent of variations that might be introduced during wafer fabrication. Also, fabrication processes usually scramble the wafer order, so that spatial information about the block is lost by the time the solar cell efficiency is determined.

A detailed view of the sense head is shown in Fig. 8. This arrangement, with a thin line of illumination, was optimized for the block-scan application. The long line averages over about ¼ of the width of the block. The thin dimension of the line is in the direction of the scan. Some data from a line scan is shown in Fig. 10. The transition between material that is suitable for fabricating solar cells, and material destined for re-cycling is fairly abrupt. The 2 mm resolution, coupled with a 1-2 mm step size will yield information sufficient to specify a cut to an accuracy of less than a millimeter.

Fig. 7 shows the apparatus after a line scan. The data is on screen, and shows the lifetime as a function of position, as well as the resistivity as a function of position. Another view of the instrument is shown in Fig. 9.

If desired, the instrument can do raster scans to accomplish a 2-D mapping. The present prototype is not automated for scanning in the second dimension, although a manual stage movement is incorporated in this 2nd axis. Extensive work on this block tester was accomplished during Phase II of this subcontract and is discussed later in this report.

As with the Solar CZ measurement, the preferred methodology of measurement and analysis with this equipment is the QSSPC method. Infra-red light creates photogeneration that extends into the silicon beyond a diffusion length from the surface. PC1D simulations give a good approximate calibration for the difference between "measured" and actual lifetime(17,21). A final correlation will probably be done by the industrial customer, by comparing the measured lifetimes to the resulting final solar cell efficiencies in order to map the complex relationship between the lifetimes as measured on as-grown materials with this method and the final solar cell efficiencies(6). Since the properties of the silicon wafer will change during high-temperature processing, the relationship between as-grown lifetime and final lifetime will be complex.

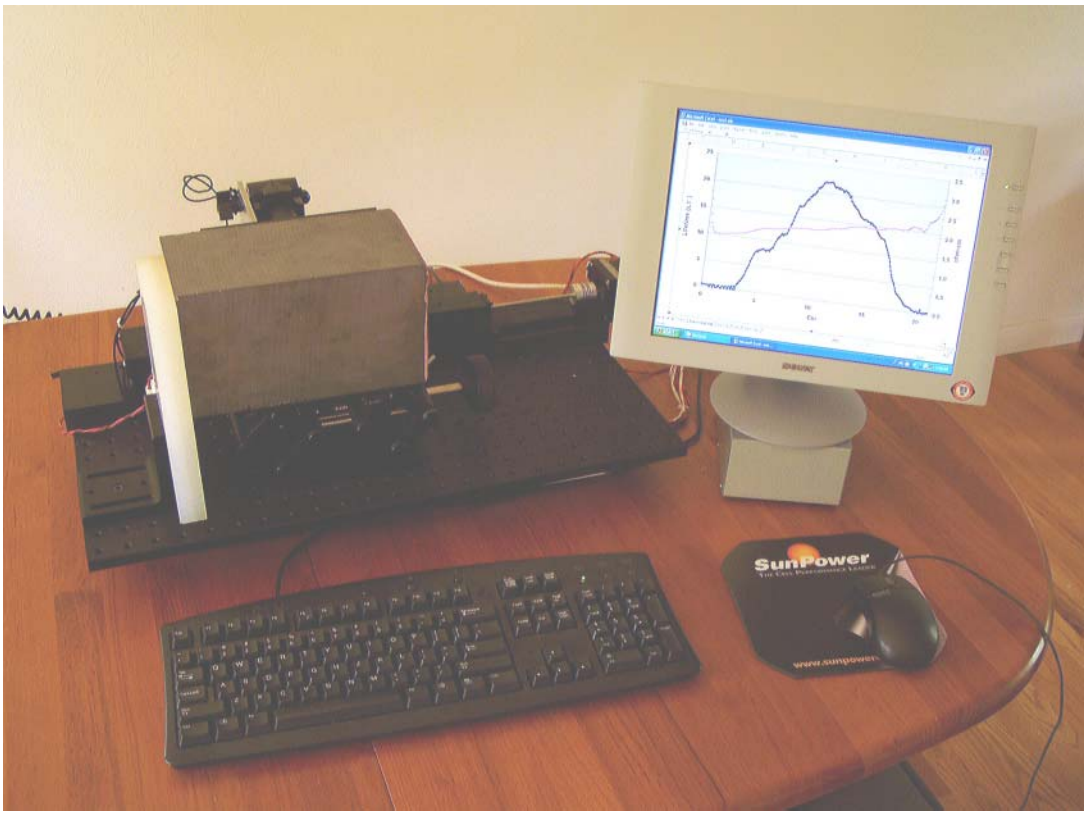

Fig. 7. This instrument performs line scans down the length of a Multi-crystalline silicon block. The sample head, (behind the block) is run along a computer-controlled stage.

Fig. 8. A detail of the block scanner, the sense head. This spot size is about 3 mm wide, and 30 mm high giving high resolution when stepped in the long (growth) axis of the block. The result is averaged over 30 mm in the axis perpendicular to the growth direction. The total illuminated area is large enough to give very good signal to noise.

Fig. 9. A different view of the block scanner indicating the sample head as it scans the block.

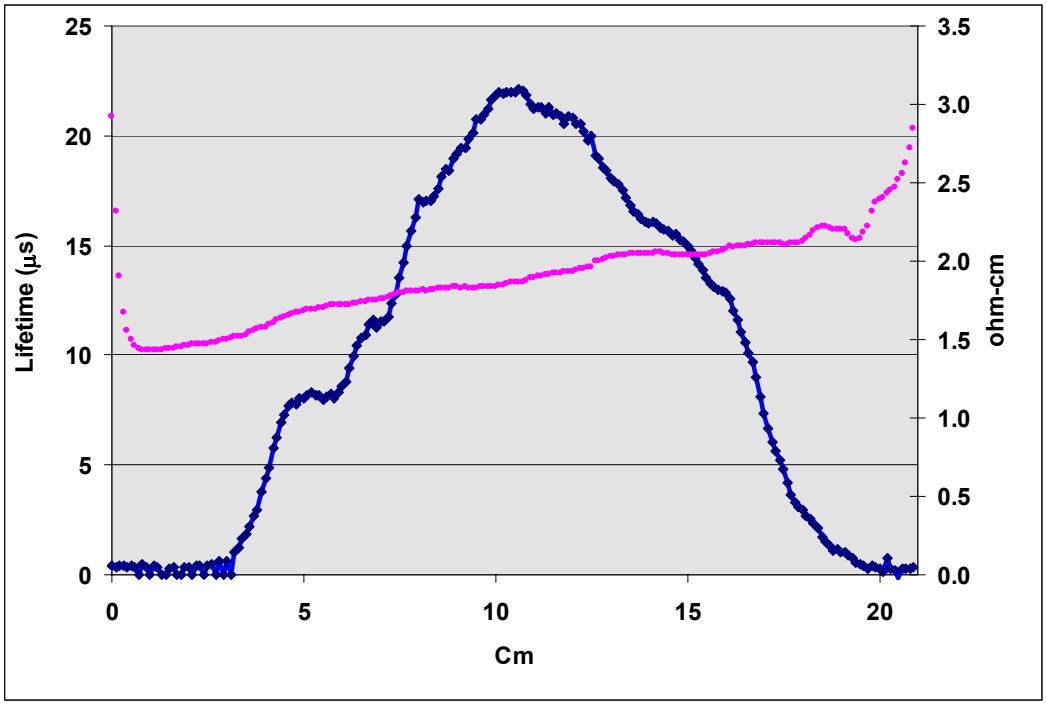

Fig. 10. A line scan. This data averages over 30 mm, about ¼ of the block width, yet has a 2-3 mm resolution in the growth direction. This data was taken at a 1 mm step size in the growth direction. Lifetime is in blue (left axis), resistivity in pink (right axis).

An Instrument for Measuring Lifetime on High-Lifetime FZ Boules

This application is unique for the series of instruments, in that it utilized the transient PCD technique. In contrast to the QSSPC technique, for a transient measurement the light is abruptly terminated, and then the decay of the photoconductance in the dark is monitored. Data taken in this way is shown in Fig. 11.

This is the optimal situation for FZ silicon. This silicon typically has very high lifetime. Recombination at the surface would have a major effect on the measured lifetime of this material as determined by the QSSPC technique. By terminating the light abruptly, the surface recombination quickly eliminates electrons from near the surface. After this initial rapid decay, the measured lifetime asymptotically approaches the actual bulk lifetime. PC-1D simulations have been applied to verify this behavior and to study it in detail (22,26).

An instrument measuring an FZ boule is shown in Fig. 13. The instrument is nominally the same as the CZ instrument. However, the analysis is different, with an optimization for this high-lifetime material. In addition, more light of shorter wavelengths is used in the excitation to obtain the highest possible initial photoconductance, since the surface modes are allowed to decay away before the bulk lifetime is determined (4,22,26).

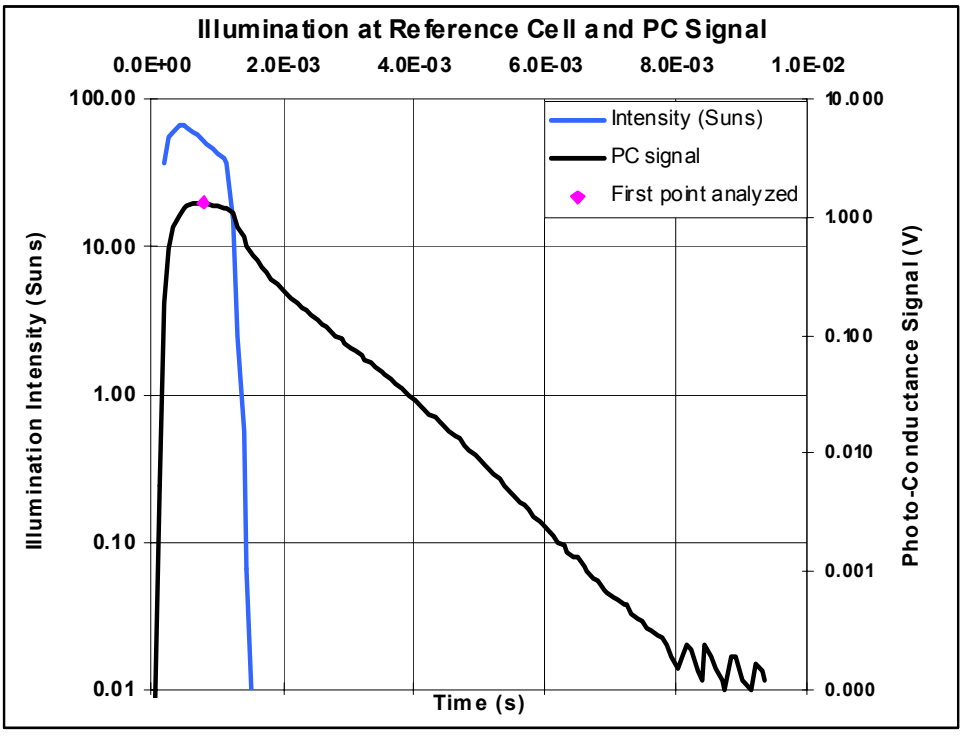

Fig. 11. A transient measurement on a 1.6 Ohm-cm p-type FZ boule of silicon. (sample courtesy of Jan Vedde, Topsil A/S).

Data from an 1.6 Ohm-cm p-type boule is shown in Fig. 11. In contrast to measurements on wafers, it is difficult to calibrate the injection-level scale precisely, since the carriers are not confined. They can diffuse deep into the bulk away from the RF sense head. This effect is a

function of the diffusion length. As a result, the minority-carrier injection levels shown on the x axis are approximate. We estimate this uncertainty to be approximately a factor of 2 in most cases.

At high injection levels, (which occur just after the light is extinguished), the measured lifetime is short as the surface recombination quickly annihilates the electrons near the surface. Boron-doped p-type material generally has lower lifetime at low injection levels than at higher injection, due to the bulk recombination. The competition between these trends leads to a maximum lifetime during this measurement at moderate carrier density. This lifetime, 1.4 ms for this boule, indicates that very long lifetime can be characterized despite the lack of surface passivation on the boule.

This instrument and measurement promises instant feedback to the grower for optimization of the material growth. In addition, it allows for specification of the boule for lifetime as a characteristic that can be given to the solar cell fabrication line or wafer customer. The layout of this instrument, with a boule to be measured, is shown in Fig. 13.

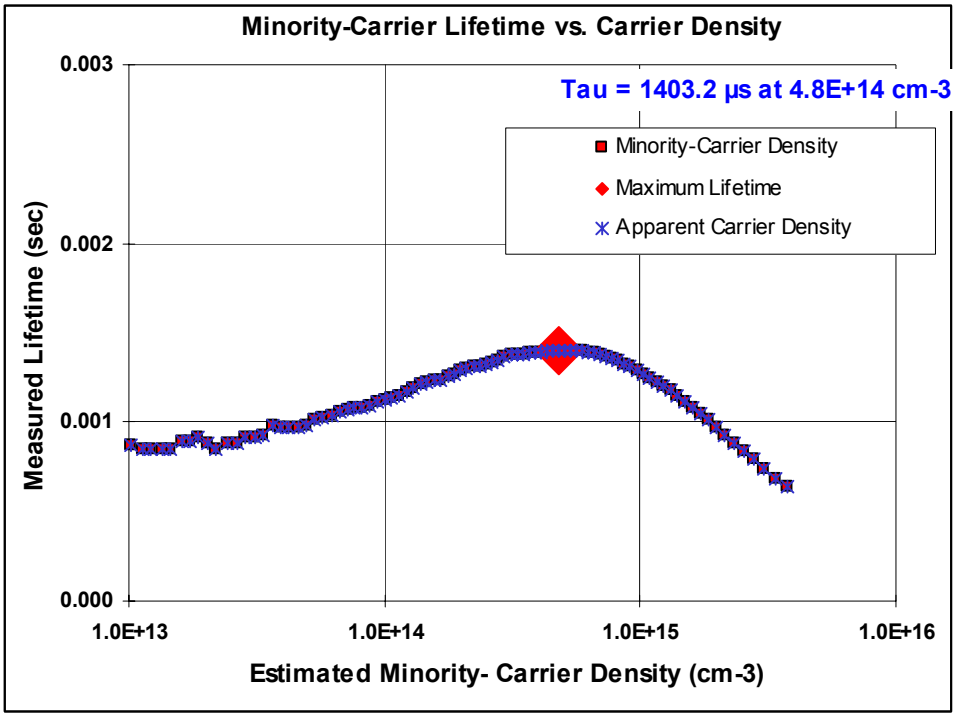

Fig. 12. Analyzed data from a transient measurement of a 1.6 Ohm-cm FZ boule of silicon. Despite a lack of an surface preparation, lifetimes exceeding 1 ms can be measured. The accuracy of the measurement results has been modeled in PC1D and detailed in an application note(26) and publication(22).

Fig. 13. An instrument that was optimized for measurements on as-grown boules of high-lifetime float-zone silicon. (Photograph courtesy of Jan Vedde, Topsil A/S).

An Instrument for the Rapid In-Line Measurement of Wafers.

The last instrument to be discussed here is a small sample head that was optimized for measuring wafers. This instrument is shown in Fig. 14. Again, for ease of automation, the internal light source configuration was used in contrast to the open-air method for the R&D instrument. However, this small sample head has a large illuminated sense area for very high sensitivity. This will allow for the measurement of unpassivated thin wafers. This case, unpassivated wafers with no surface recombination, is quite difficult to measure due to low effective lifetimes in the wafers, coupled with highly-variable levels of trapping, which tends to bury the signal that would be due to minority-carrier photoconductance(11).

This instrument applies a correction for trapping that is based on obtaining the full injection-level dependence of the measured lifetime(11). In addition, the wavelength dependence of the lifetime has been applied to better separate out the surface from the bulk effects in order to more accurately track the bulk lifetime(1,17). This was reported at the PVSEC in Osaka(17), detailed in an application note(11), and summarized in the first annual report on this contract(23). For the case of typical industrial solar cell wafers, (300-μm-thick, 1 ohm-cm p-type wafers) guidelines for QSSPC measurement have recently been detailed in a handbook form(7). When extensive data became available from industry in the 2nd phase of this contract, we revisited this problem with a fully numerical solution that could incorporate the spectral distribution of our light sources. This new analysis supersedes the original one and is described later in this report.

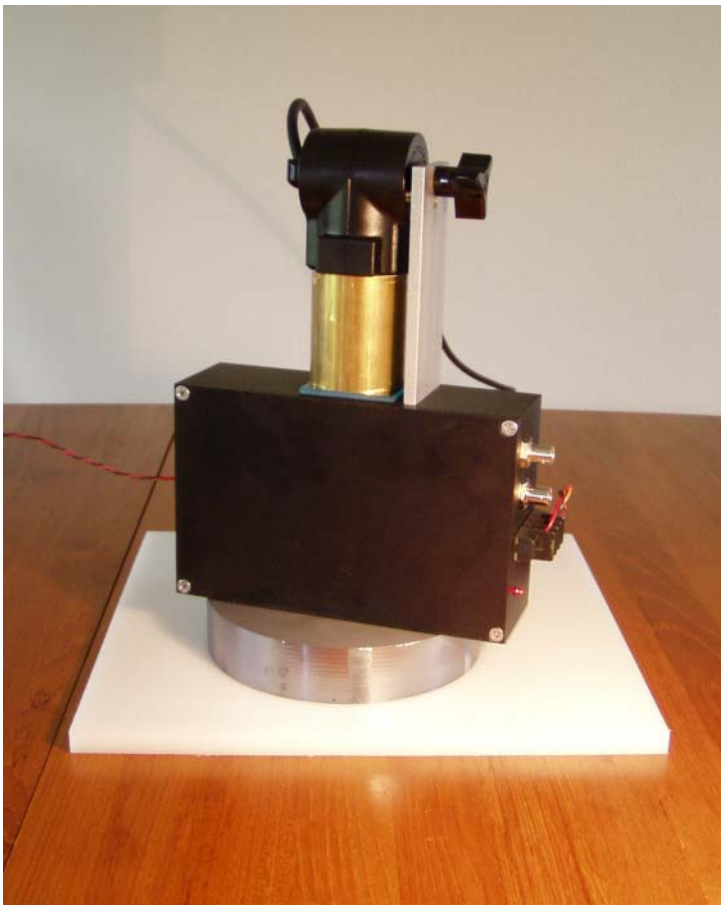

Fig. 14. This sample head is optimized for in-line measurements of wafers or flat surfaces of uniform blocks. The illuminated area is large, to enable high sensitivity for measuring unpassivated wafers just entering the process line, and giving very one-dimensional results on phosphorus-diffused wafers.

Two application notes were developed for the instrument in Fig. 14. The first is coupled with a special version of the software analysis, and is optimized for bare wafers(27).

The second application note is focused on measuring wafers after the phosphorus diffusion(24). There is already ample data from industry using the WCT-100 R&D instrument that the lifetime measured after the phosphorus diffusion is very predictive of the final solar cell efficiency. This measurement has been used to qualify both the process and the wafer at this stage, where the cost of screen print and final test can still be avoided if the wafer or emitter diffusion is bad. Also, any process problems can be quickly identified almost as soon as they occur giving unambiguous feedback very close to the source of the problem.

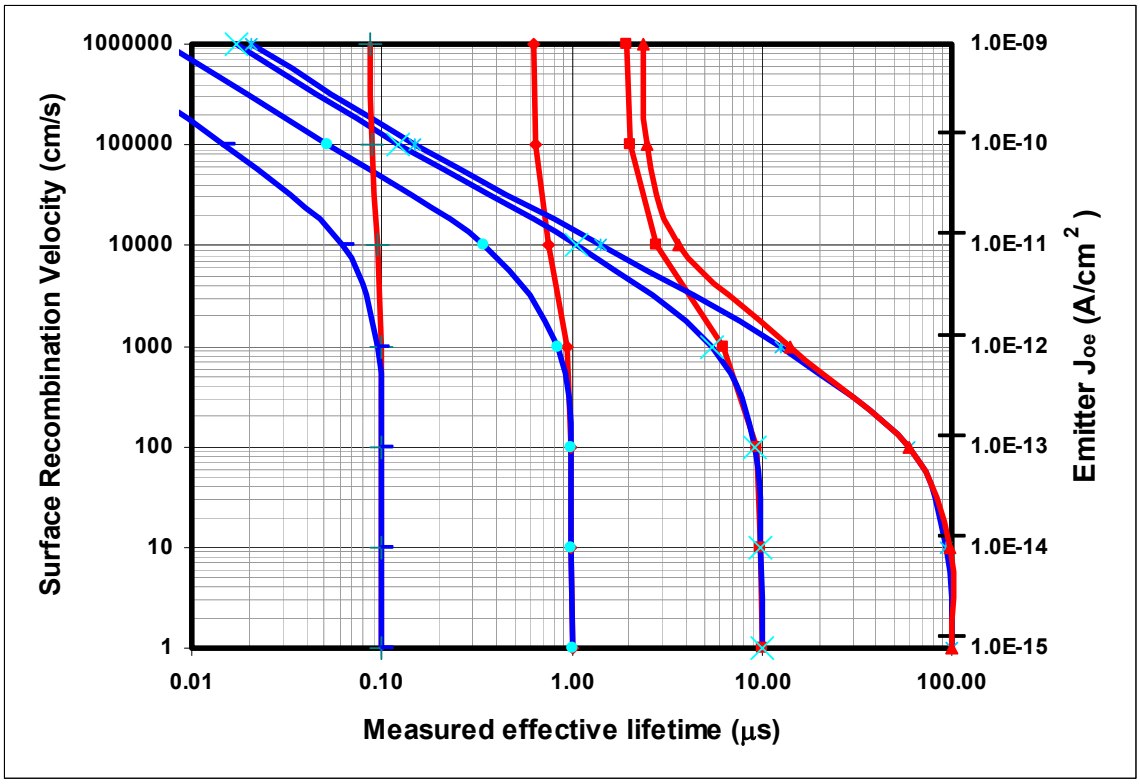

Fig. 15. The wavelength dependence of photoconductance has proven to be a powerful tool in R&D. These curves indicate the different lifetimes that would be measured on industrial 1 ohm-cm, p-type substrates with bulk lifetime of 0.1, 1, 10, and 100 μs, as a function of the surface recombination. For well passivated wafers, the measured lifetime is the bulk lifetime. For unpassivated wafers, the difference between the lifetime measured under blue and infra-red light can be used to accurately determine bulk lifetime and surface recombination velocity(1,7,17).

Task 3. Develop Application Notes for Industrial Use of Lifetime Testing in the Production Line

The intent of this task was to develop application notes for industrial applications of the instrument. These notes should operate on several levels. First, they should allow a simple procedure to obtain immediate and valid results. Second, they should provide an explanation of the device physics connecting the measurement procedure and results solidly to the scientific basis for the measurement.

These notes have been completed for 4 applications:

1) Measurements on bare wafers(27). A special version of the software was constructed that is optimized to be very robust for this measurement. The application note details the basis for the measurement. The technique chosen for this optimization involves the spectral response of the measured lifetime to correct for the high-surface recombination velocity. The study and qualification of this technique was reported in a conference paper(17). A more complete and updated version was developed in Phase II of this subcontract and is discussed under Task 5 in this report as well as in Ref. (28).

2) Measurements on relatively uniform blocks or boules of material. An application note details both the use of an optimized instrument and QSSPC to measure CZ solar silicon, and the use of transient PCD for measurements on FZ silicon. Some details of the QSSPC measurement were presented in a conference paper(11). The FZ analysis is as yet unpublished other than the application note itself(8).

3) Measurements on wafers after phosphorus diffusion, or after other good surface passivations. This application note(24) focuses primarily on the optimum measurement strategies for industrial wafers after the phosphorus diffusion, but has general discussion of other wafer types as well. The use of high-resistivity wafers to qualify a diffusion process is also covered. Some details that are particular to multi-crystalline wafers, and the interpretation of data from wafers with widely varying grain lifetimes was presented in a conference paper(18). This paper discusses the type of lifetime average that results from the circuit connection through the junction that is present during measurements on wafers after the phosphorus diffusion.

The function of measuring sheet resistance or resistivity with the conductance sensor in these instruments has been formalized in two applications. In the block scanner, this resistivity is measured and plotted as a function of position. For the wafer measurement tools, this function has been implemented so that the measurement is taken automatically whenever a lifetime is measured.

Phase II. 15 Months Starting August 2003

In this phase, the results of the first year were consolidated into industrial instruments. In addition to the technical aspects of developing the new instruments, great effort was put into future-looking applications that would speed the adoption of the new tools within industry.

A new user interface was introduced for use on all of the tools. This interface replaced all of the references to the previous oscilloscope-based system, which required the user to understand "AC" vs. "DC" coupling, trigger levels, horizontal and vertical scales and positions, etc. Instead, the user zooms in or out on the data as if it were a mapping program on the internet. Zooming in gives more detail on a small subset of the data taken, while zooming out displays all of the data (with less detail). The computer optimizes the detailed data acquisition parameters in the background. An expert system guides the user to a good measurement. The result of this new interface is that the training time for new users should be greatly reduced. The expert system also met the goals for a fully-automated system that runs without user intervention.

While the description of Phase I of this work was in large part organized around 4 instruments with some results from each, Phase II was largely driven by the development of unique, leading edge industrial applications of the new tools. The instrument modifications were done in support of the development of these applications. Therefore, this Phase II report focuses on two of the most important developments of this work. These are the measurements of as-cut wafers directly on a production line before any processing, and the measurements on bricks of silicon prior to slicing into wafers. These are reported under Task 6 below, and form the centerpiece of the work.

Task 4. Engineer the Integration of Discrete Components into a Stand-Alone Instrument

Several instruments were fabricated specifically for each application of interest. These will be discussed in the next section, in the context of their application. All of the technical aspects of each instrument were optimized for the specific application. In addition to the technical feasibility of the measurement, in each case we designed and tested instruments to be capable of measuring at a rate equivalent to one wafer per 2 seconds, including logging of all of the relevant data to a database.

In May of 2004, an instrument was delivered to NREL for use in their laboratory research. This instrument was of the type shown in Fig. 14. This would be the most useful instrument for NREL, in that it can be used for boules of high-lifetime silicon, as well as multicrystalline bricks or wafers. This new instrument included the new hardware and user interface developed in this work, as well as the latest application notes for measuring wafers of all types as well as blocks or boules of silicon using transient or quasi-steady-state measurement methodologies.

Task 5. Finalize and Document Application Notes for a New Sample-head Instrument

Two of our new applications are discussed in this section, the measurement of as-cut bare wafers and the mapping of lifetime, Fe concentration, and trapping effects in bricks of multicrystalline silicon. The first topic was presented at the NREL silicon workshop(28). The second topic was presented in Paris at the European conference and further discussed at the NREL workshop(2,21,22,).

The Measurement of As-Cut Un-Passivated Multicrystalline Wafers

Introduction

In the silicon solar cell industry, as-cut wafers are often purchased for use in production. The complete characterization of these wafers at this point of sale is a desirable goal. Processing wafers that are not destined to yield product wastes production capacity in the cell manufacturing line. Not processing wafers that could yield good solar cells wastes the value of the ingot growth, brick preparation and sawing of those wafers. This application presents a methodology for measuring unprocessed, bare wafers using the Quasi-steady-state photoconductance (QSSPC) technique in order to estimate the bulk lifetime despite the overwhelming effect of high surface recombination velocity on unpassivated wafers. These topics were presented in technical paper at the European conference in Paris(21) and the NREL silicon workshop(28).

Methodology

For typical incoming bare multicrystalline wafers, the following issues need to be addressed.

- Since the surfaces are unpassivated, the maximum lifetime that will be measured is quite low, less than 3 μs. This can lead to poor signal to noise ratio [15].
- Trapping effects can give artificially high apparent lifetimes, especially because the surface recombination limits the signal due to the fact that the minority-carrier concentration, and hence the associated photoconductance, is relatively low [9]. Trapping results in a spurious conductance term that is due to majority carriers and therefore unrelated to the recombination lifetime.
- Because the behavior can be dominated by trapping, the photoconductance signal amplitude and shape is quite unpredictable. This creates difficulty with respect to finding a data analysis that works well for ratios of trapping conductance to minority-carrier conductance that can vary over orders of magnitude.

The analysis of bare wafers using the QSSPC technique was made robust with the following optimizations:

1) The minority-carrier density to evaluate the lifetime is fixed at 85% of the maximum carrier density achievable with the light source (flash plus filter). This insures good signal to noise, although it means that data for different wafers is evaluated at different carrier densities. An alternative is to use a fixed minority-carrier density when the signal is adequate, yet use the above rule when the signal is small.
2) Bias light was used to correct for trapping. Most bare multiX wafers have the behavior where the correction is rather independent of bias light beyond a certain bias light level [11]. Normally, 2-10 suns of bias light will give good results for the full range of trapping even into the rather extreme cases.
3) An infra-red-pass Schott-glass filter (RG-850) is used to insure nearly uniform generation deep within the wafer. Although an even longer wavelength (such as the RG-1000 filter shown in Fig. 21) would be desirable for better uniformity, the 850nm filter offers a better compromise to maintain a high photon flux.

For nominally 1-ohm-cm p-type bare wafers, the surface recombination velocity is very high and relatively well known. As a result, a correction can be made on the final data based on the measured lifetime and the wafer thickness. Previously, we investigated the surface recombination velocity of 1-ohm-cm p-type wafers and found it to be approximately 2 x 10^5 cm/s[4], which places it close to the kinetic limit. In this limit the carrier density at the surfaces is extremely small and negligible compared to the carrier density within the wafer. This assumption of high surface recombination velocity can be checked at any time by performing a lifetime measurement with visible light[1,7].

For perfectly uniform photogeneration and infinite surface recombination velocity it is possible to derive analytically the following relationship between the actual bulk lifetime and the measured effective lifetime [28]:

$$\tau_{eff} = \tau\left(1 - \frac{2L}{W}\tanh(\frac{W}{2L})\right) \quad \text{Eq. 1}$$

where τ is the bulk lifetime, L is the diffusion length, and W is the wafer thickness.

The Sinton Consulting instruments use a Xenon flash with Schott glass filters. The spectrum for the flash has been measured at NREL, and the filter specifications are known. The PC1D simulation program[3] has been used to determine a relationship analogous to equation Eq. 1 for the practical application using infrared light from the xenon lamp and filters[13].

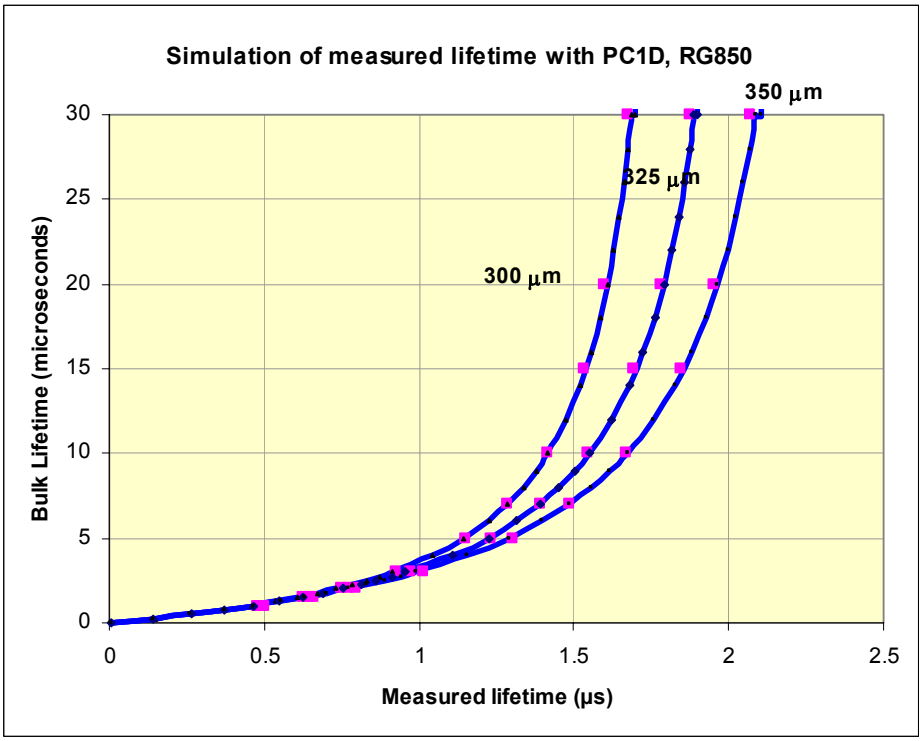

Fig. 16. The function to convert measured lifetime to bulk lifetime for the Sinton QSSPC measurements with the Schott-glass RG-850 filter.

These numerically-derived results can be fit with an equation that is analogous to the Eq. 1.

$$\tau_{eff} = A\tau\left(1 - \frac{2L}{W}\tanh(\frac{W}{2L})\right) \quad \text{Eq. 2}$$

Where the factor "A" is a function of the Schott filter type and the wafer thickness. For the 850 nm IR-pass filter,

$A = 440W^2 - 37.5\ W + 1.44$

W is the wafer thickness in cm. This fit is shown for the 300, 325 and 350 micron-thick simulation in Fig. 4. Notice that a measured lifetime of 1.5 μs would correspond to about 7 μs if the wafer were 350 microns thick, but about 13 μs if the wafer were 300 microns thick. This fit is valid only for the limited range shown here. For the full range, the original numerical curve can be used.

Fig. 17 shows an expanded version of Fig. 16. For a 325 micron-thick wafer, a measured lifetime of 0.8 μs corresponds to a bulk lifetime of 2 μs. A measured lifetime of 1.5 μs corresponds to a 9 μs bulk lifetime. For high bulk lifetimes, small uncertainties in the measured lifetime become large uncertainties in the bulk lifetime. As expected, this is especially true for thinner wafers. In the thin limit, the measured lifetime is completely determined by the surface

recombination and transport parameters rather than bulk lifetime. The curves shown in Fig. 16 and 17 were calculated numerically for the photon distribution particular to the Schott-glass 850 nm IR pass filter, as shown in Fig. 18.

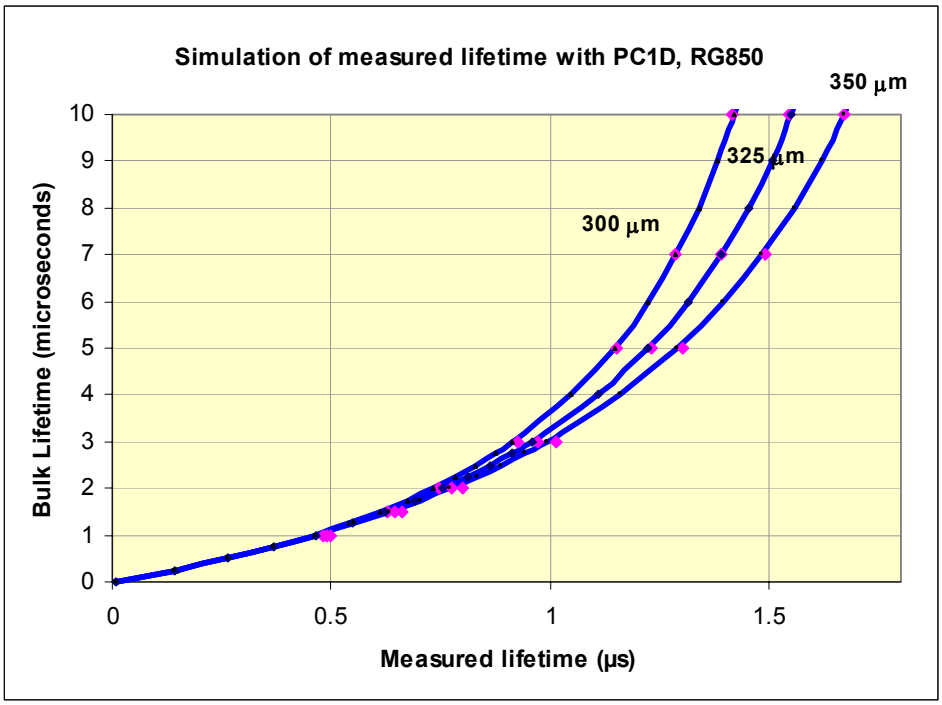

Fig. 17. The PC1D simulations for conversion of measured to bulk lifetime. The diamonds are the PC1D points, the lines are fits using eq. 2.

The conversion of measured to actual lifetime proposed here is different than in the recent paper that we presented in Osaka. In that paper, we proposed that for uniform generation, the correction would be[17]:

$$\tau_{\text{bulk } QSSPC}^{-1} = \tau_{measusred\ QSSPC}^{-1} - \tau_s^{-1} \quad \textbf{Eq. 3}$$

that might be taken to imply that

$$\tau_{\text{bulk } QSSPC}^{-1} = \tau_{measusred\ QSSPC}^{-1} - \frac{12 D_n}{W^2} \quad \textbf{Eq. 4}$$

which is **incorrect** for the QSSPC case, except when the diffusion length is extremely high. This became clear in the numerical simulations for this work, and has been verified using the analytical equations as well[2]. Unlike the transient case, for steady-state measurements the surface recombination lifetime term is a function of the bulk lifetime. In the low-lifetime regime, with L<W, the above QSSPC equation would result in a 15% error in the calculated bulk lifetime.

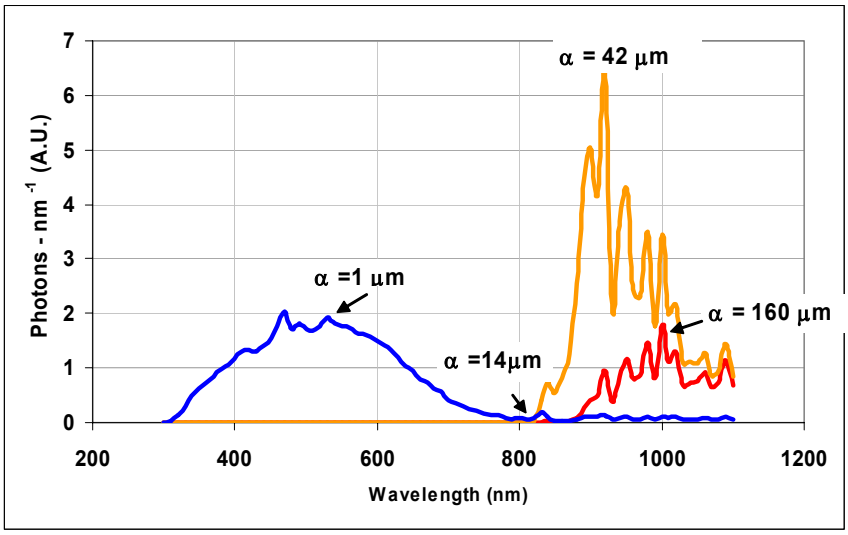

Fig. 18. The photon distribution from a Quantum flash through 3 Schott-glass filters, the BG-38,RG-850 and RG-1000.

The fact that the surface lifetime is not independent of the bulk lifetime is illustrated in Fig.19. Surface recombination can only impact the electron concentration for a few diffusion lengths from the surface. For long lifetimes, with L>>W, the surface recombination will determine the shape of the carrier concentration throughout the wafer. This is similar to the case for transient photoconductance measurements. This case is shown in the left of Fig. 18. However, in cases where L << W, the shape of the carrier density is much different as shown in the right graph in Fig. 19. Here, for a wafer with 1 µs bulk lifetime, the carrier density is determined mostly by the bulk lifetime except for within a few diffusion lengths of the surface. Clearly, the carrier density can be quite large near the surface, leading to a lower surface lifetime. This function is shown in Fig. 20, and indicates that Eq. 4 is accurate only when L>>W.

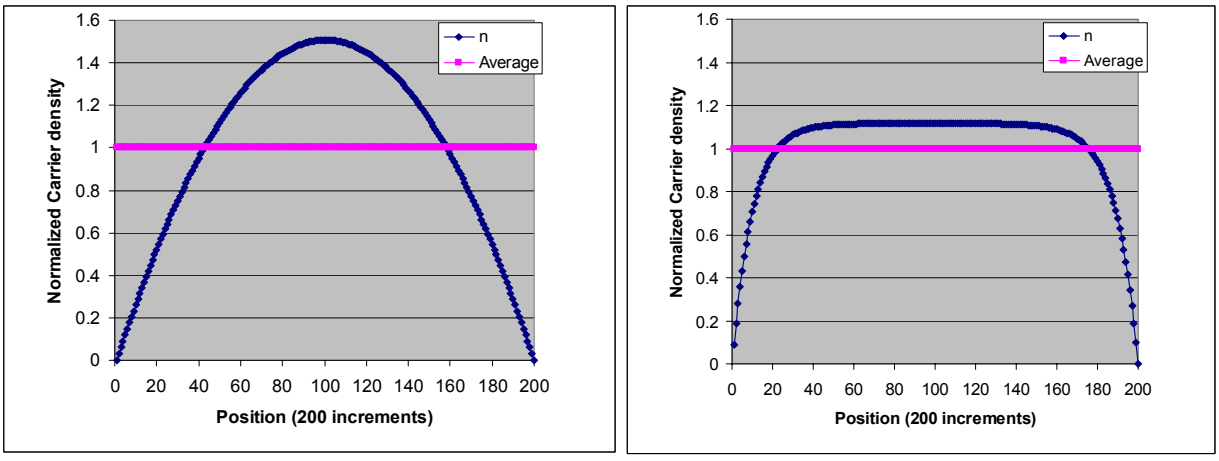

Fig. 19. A comparison of the shapes of the carrier density profiles under steady-state illumination with uniformly absorbed light. A wafer with 1 ms bulk lifetime (left) is compared to a wafer with 0.1 µs lifetime (right). For L<<W, (right), the average position of the carriers is much closer to the surface, leading to a lower surface lifetime as indicated in Fig.20.

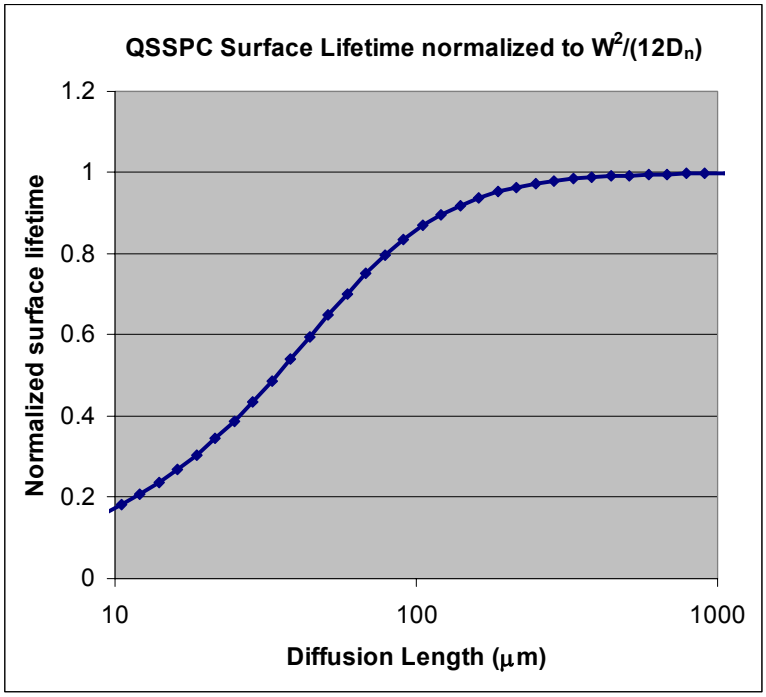

Fig. 20. The surface lifetime for an unpassivated wafer measured with uniformly-generated light compared with the asymptotic limit for high-diffusion length.

Practical Application

An application of this lifetime testing methodology is shown in Fig. 21 and 22, where the measured lifetime, resistivity, and trap conductance are shown for 400 sequentially-measured wafers in the original order in which they were grown in the brick. These wafers have no surface passivation. Fig. 21 shows a new version of the small sample-head lifetime tester designed for in-line lifetime testing. In contrast to the relatively small sampling shown in the original version in Fig. 14, industrial customers wanted a large-area sensor. The new instrument shown in Fig. 21 measures the area-averaged lifetime over an 8-cm diameter. When each wafer from a block is measured sequentially, the effect is as shown in Fig. 22, where a cylindrical core of material right down the center of the block has been characterized.

Fig. 21. A sample head that can be mounted in a production line to measure every wafer. The measurement area is an 8-cm diameter.

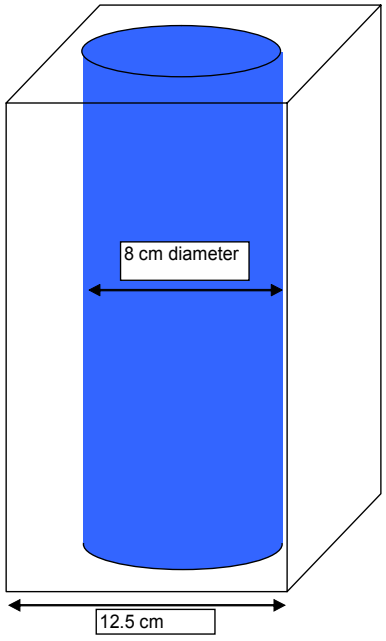

Fig. 22. A diagram indicating the volume of a block of multicrystalline silicon that is measured one wafer at a time by measuring 400 wafers from the block sequentially.

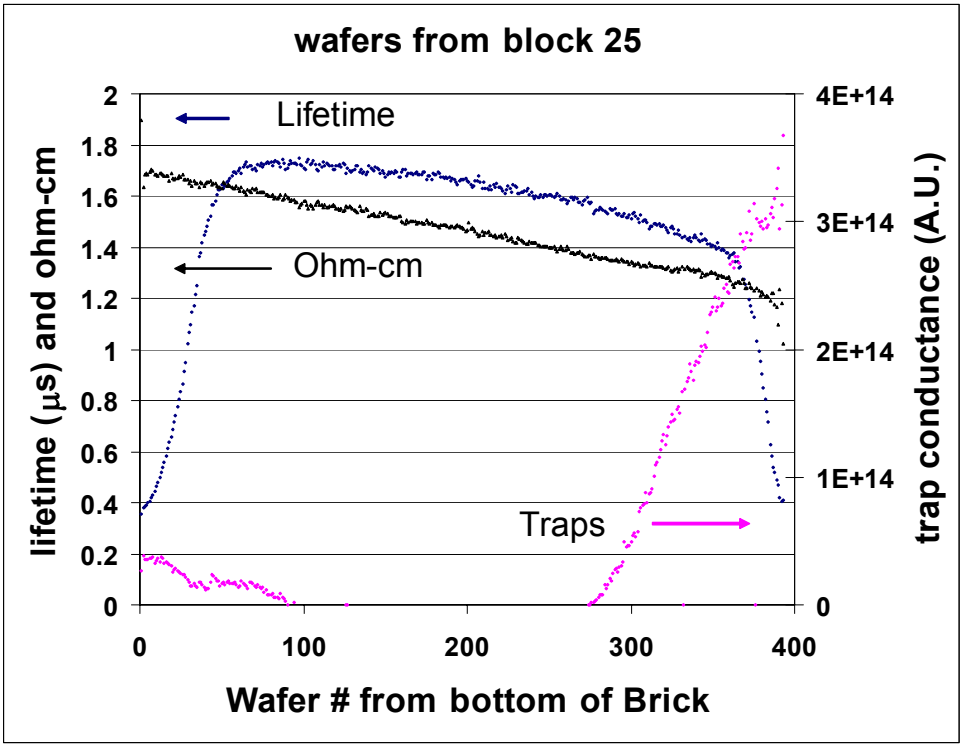

Fig. 23. The measured lifetime for 400 sequential wafers from a corner brick from a multicrystalline ingot. The measured resistivity and trapping conductance is also shown.

The measured lifetime for a corner block of silicon shown in Fig. 23 is surprisingly smooth, with little random noise apparent in the measurement. The lifetime from wafer 1 at the bottom of the brick to wafer 400 at the top shows the trends expected based on typical block measurements, with the low lifetimes at both ends, and the highest lifetime in the middle of the brick on the side towards the bottom of the brick[8].

Although the minority-carrier photoconductance is capped to be less than 2 μs by the overwhelming effect of the surface recombination velocity on the measured lifetime, the trapping photoconductance (a majority carrier effect) should be the same on passivated or unpassivated wafers. Therefore, it should be very interesting to search for clues in this trapping data that correlate to cell performance. Accurate tracking of trapping in wafers should not require surface passivation.

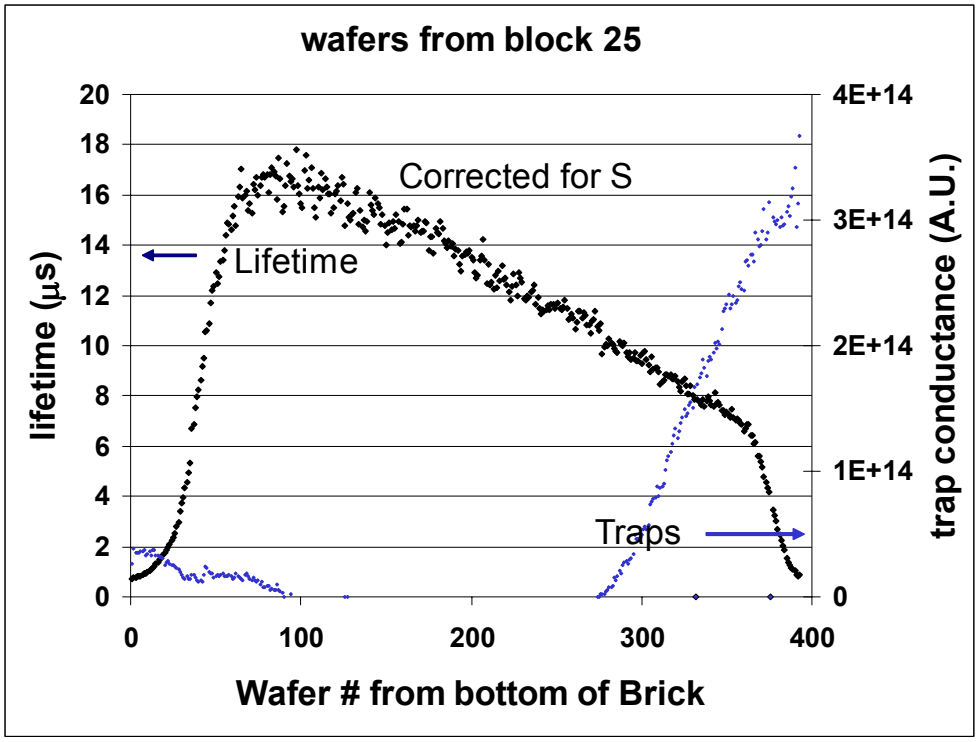

Fig. 24. The estimated bulk lifetime based on the data from Fig. 7., 325-µm nominal wafer thickness and equation 2.

Figure 24 shows the bulk lifetime for these 400 wafers as calculated from eq. 2. This procedure essentially removes the 2-µs ceiling imposed by surface recombination in Fig. 23, indicating that the bulk lifetime in parts of this block was greater than 15 µs.. These lifetimes should correspond to a calibrated measurement done on the block, or to measurements done on these same wafers with surface passivation. This further experiment was not performed on these wafers at this time.

From Fig. 16 and 17, it is clear that for calculated bulk lifetimes greater than 10 µs, small uncertainties in the measured lifetime translate to large uncertainties in the bulk lifetime. In practice, these errors could be minimized by measuring the thickness of each wafer instead of using a nominal thickness. The use of reference wafers with high bulk lifetime could verify the correction. If the correction is resulting in systematic errors towards high lifetime, then a known high-lifetime wafer would measure infinite or negative lifetime from Equation 2.

In the range of bulk lifetime that is critical to the decision to process a wafer or not, 2-5 µs, the uncertainty in the bulk lifetime is quite small. The curve is not into the steep region where measurement uncertainties translate into large bulk-lifetime uncertainties.

One overall conclusion from data such as that in Fig. 24 is that context is important. It seems likely that good blocks have a characteristic profile of trapping and minority carrier lifetime. Judging wafer lifetime and trapping data relative to the expected result for a particular wafer number should give a much better decision than the absolute values for the lifetime and trapping

for any particular wafer. Correlation of these results, wafer position, lifetime, and trapping with final solar cell efficiency will be required to validate various models to determine "passing" and "failing" values for wafers.

Several weaknesses in this analysis should be pointed out for future study. If the lifetime measurements as proposed here are done before wafer etch to remove surface damage, this may result in reported lifetime that is lower than the actual bulk lifetime. This is due to the uncertainty in wafer thickness due to the penetration extent of the saw damage. Secondly, the analysis to convert measured to bulk lifetime presented in this application assumes a homogeneous lifetime across the wafer. This is a clear limitation of any technique for multicrystalline wafers short of a full 2-dimensinal mapping followed by a comprehensive analysis of each pixel and appropriate weighting over the full wafer to get the final result. Future work will indicate if these are significant effects.

Conclusions

A methodology for estimating the bulk lifetime based on the measured lifetime of 1 ohm-cm p-type wafers has been developed. With the use of numerical modeling, the correspondence between measured and bulk lifetime has been found for the spectral distribution of light used in the measurements. This allows the measured data to be converted to estimated bulk lifetime. By using the QSSPC technique, the effects of trapping can be tracked and corrected for in the lifetime data.

Initial data taken on all of the wafers from multicrystalline bricks resulted in characteristic traces of the lifetime and trap conductance profiles as typically seen in data taken on bricks before sawing. There is little random noise in the data. Further work may establish the correlations between wafer position, bulk lifetime, trapping, and final cell efficiency to enable this technique for use in wide-scale process-control applications.

Evaluating Multicrystalline Bricks for Lifetime, Trapping, and Fe Concentration

Introduction

Most previous work using the QSSPC method has determined the area-averaged lifetime over an area of approximately 4 cm diameter on wafers. In this application, we developed spatially-resolved block measurements achieved by limiting the light to a well defined line as shown in Fig. 25. Using this line, an average lifetime is measured over the height of the line (30 mm), but a resolution of 2 mm is achieved in the width direction. This can be used for lines scans of multicrystalline blocks, with good resolution in the scan (growth) direction. Once the different geometry of blocks compared to wafers is taken into account, the standard QSSPC data analysis[7] can be performed on the resulting data giving the lifetime as a function of injection level. QSSPC measurements on wafers have been used to investigate trapping and Fe

concentrations as well as for the measurement of lifetime[8,10]. This application describes similar measurements taken directly on production silicon blocks.

Calibration of the QSSPC technique for use on multicrystalline blocks

The difficulty of calibrating the instrument is illustrated by Fig. 26. When doing any recombination study, it is vital to know the minority-carrier density where the lifetime is measured. The photoconductance instrument measures the total photoconductance[6]. Fig. 26 shows the minority carrier density in the surface 2 mm that results from steady-state illumination of a 1-ohm-cm p-type block of silicon. The bulk lifetime is 2μs, the surface recombination velocity is $2x10^5$ cm/s and the absorption depth of the light is 20 μm. We hypothesize that an appropriate choice for the carrier density that represents this type of distribution is given by the weighted average of the carrier density, where the weighting function is the carrier density. This gives the average carrier density seen by the average minority carrier. The resulting effective carrier density and depth is shown in Fig. 26. This is the carrier density that will be reported for a measured lifetime. In addition, since the electron mobility is dependent upon carrier density, this calculated carrier density is also used in the conversion of photoconductance to minority-carrier density.

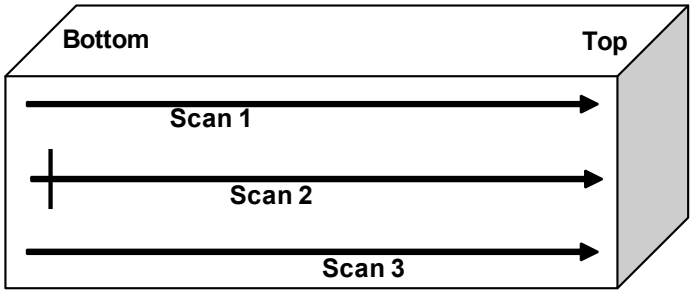

Fig. 25. The photoconductance is determined by a 3 by 30 mm illumination pattern through the sensor. This pattern is scanned across the block, giving high resolution in the growth direction. The sensor shape is shown in Fig. 8.

For this work, IR-pass filters were used in conjunction with a xenon flashlamp rather than a monochromatic source as shown in Fig. 26. As a result, the functions illustrated by Fig. 26 were evaluated using PC1D to determine the minority-carrier density profiles that result from the photon distribution of the light from the flash and filter[13].

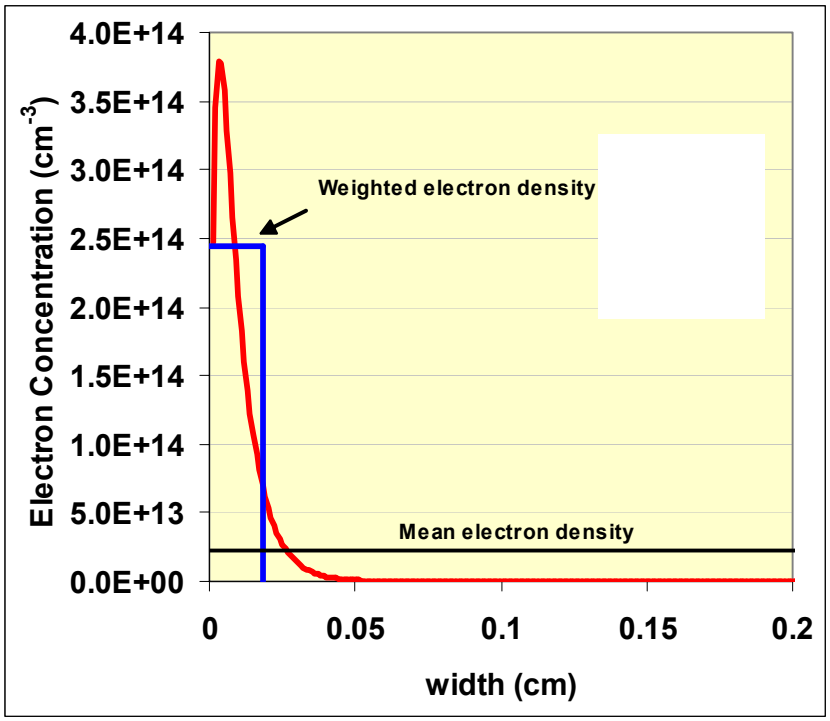

Fig. 26. An illustration of the electron carrier density profile in the top 2mm of a silicon block, and the weighted carrier density used in the analysis and reported for each measurement.

A second challenge in measuring blocks is that the surface is not passivated. The resulting high-surface re-combination will result in a measured lifetime that is much lower than the bulk lifetime. In this work, PC1D was used to evaluate the transfer function from the measured to bulk lifetime for the lifetime range and photon distribution in this experiment. This is shown in Fig. 27. This work was presented in detail at a recent workshop[2].

Measurement of Lifetime, Trapping, and Fe Concentrations.

Unfortunately, it has been shown that the lifetime of as-grown multi-crystalline silicon is often only loosely correlated with the solar cell efficiency that will result. The high temperature processing and resulting gettering both fundamentally change the material during processing. However, measurements on wafers have indicated that if the Fe concentration is measured and the effect of it is removed from the lifetime data of as-grown material, then the solar cell efficiency can be predicted with much better accuracy[8]. The method is to light-soak the wafer and determine the dissolved Fe concentration by noting the change in lifetime at a specific calibrated minority-carrier density[8,10].

The lifetime profile in a line scan along the length of a block is shown in Fig. 28. The lower curve was taken before light soaking, and the upper curve directly after light soaking for two minutes. The light soaking was done using 400W of halogen light incident on a 3-cm-wide line down the length of the block. Over the course of a few hours, the lifetime returned to the initial value. This is another characteristic of Fe in Boron-doped silicon. Both before and after light soaking, this block shows very long lifetime. For long-lifetime homogeneous material, as is evident from the QSSPC results in Figure 28, transient photoconductance measurements can be performed with the same instrument to validate the QSSPC

analysis methodology[22,26]. The resulting lifetime for the peak lifetime region of Figure 28 was 306 µs, as measured from the transient photoconductance decay.

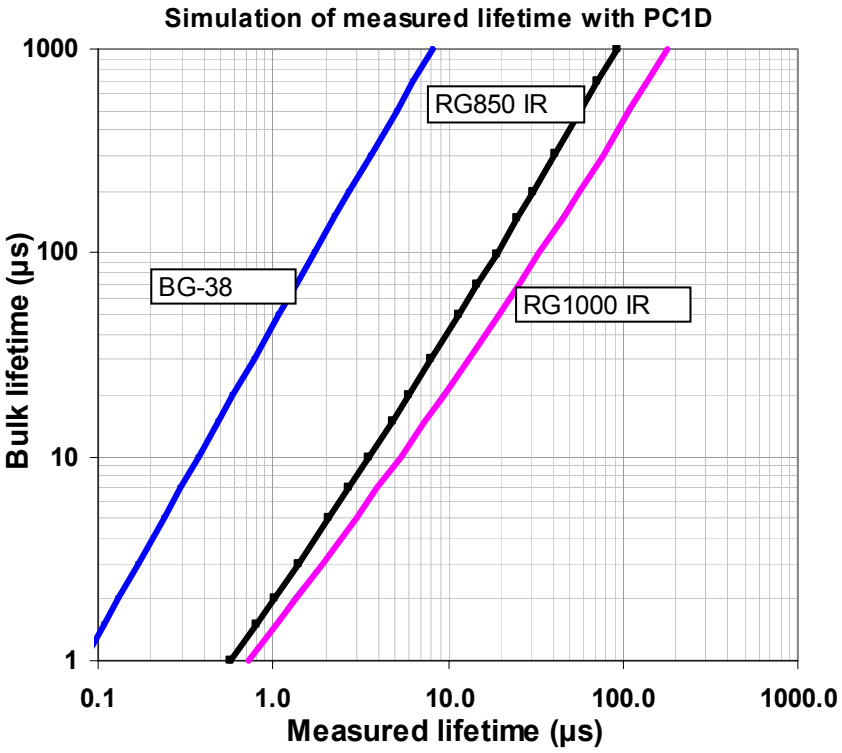

Fig. 27. The transfer function from measured lifetime to bulk lifetime as evaluated using PC1D[3] for 1 Ohm-cm p-type silicon and the photon distribution in the filtered light source(Fig. 27). Here, data from the RG-850 filter is presented.

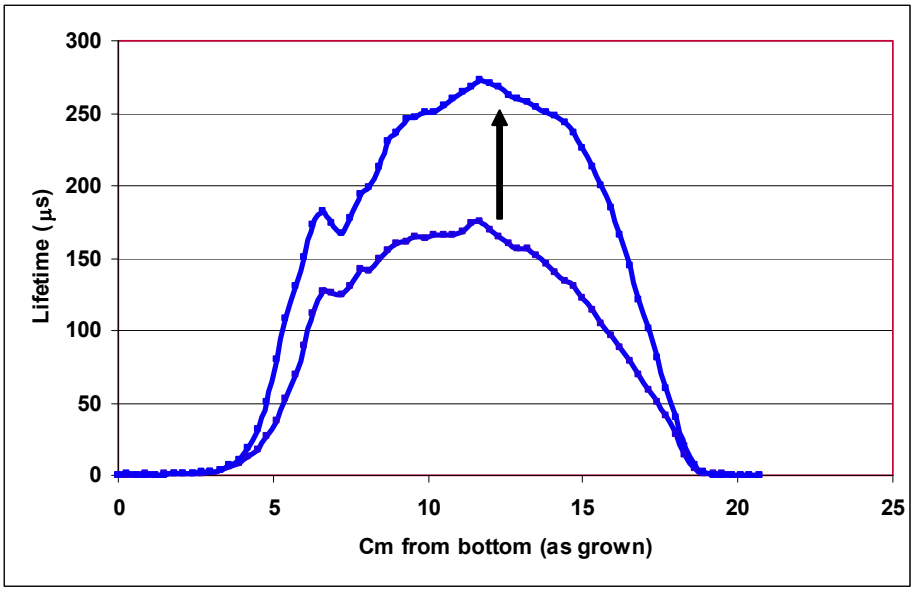

Fig. 28. A linescan along the length of a multicrystalline block directly before and after light soaking.

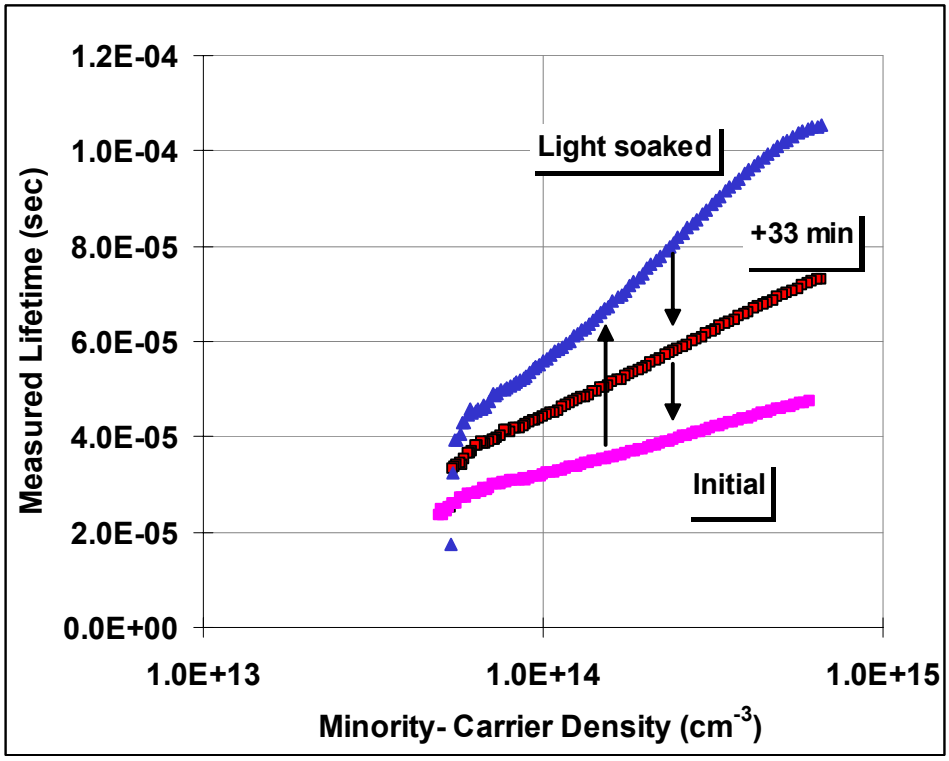

Fig. 29. The injection-level dependence of the lifetime for a particular position on the block duplicates the main features of the dependence as previously measured on wafers[10]. However, the intersection of the curves is not at the 1-2E14 value previously measured for nitride-passivated wafers[10].

The analysis of the lifetime data presented by Macdonald et al.[10] was applied to lifetime data from 6 blocks of multicrystalline silicon. The results from one face from one block are shown in Fig. 30 and 31. The lifetime after light soaking is shown in Fig. 30. The three traces correspond to the lengthwise scans as shown in Figure 25.

This Fe profile, shown in Fig. 31, shows the same main features that have been found by Geerligs[8]. He did measurements on nitride-passivated wafers from differents regions of multicrystalline blocks. For some samples, he found the profile of Fe at the bottom of the block that is due to the solid-phase diffusion of Fe up from the bottom of the ingot (left in Figure 31) during the long times at high-temperatures after this material is solidified. The increase of Fe along the block is due to the segregation of Fe into the melt during solidification, and the sudden increase at the top is highly-defected material where the remaining Fe (and other impurities) in the melt are frozen in. Some solid state diffusion "backwards" occurs giving a diffusion profile back into the top of the ingot.

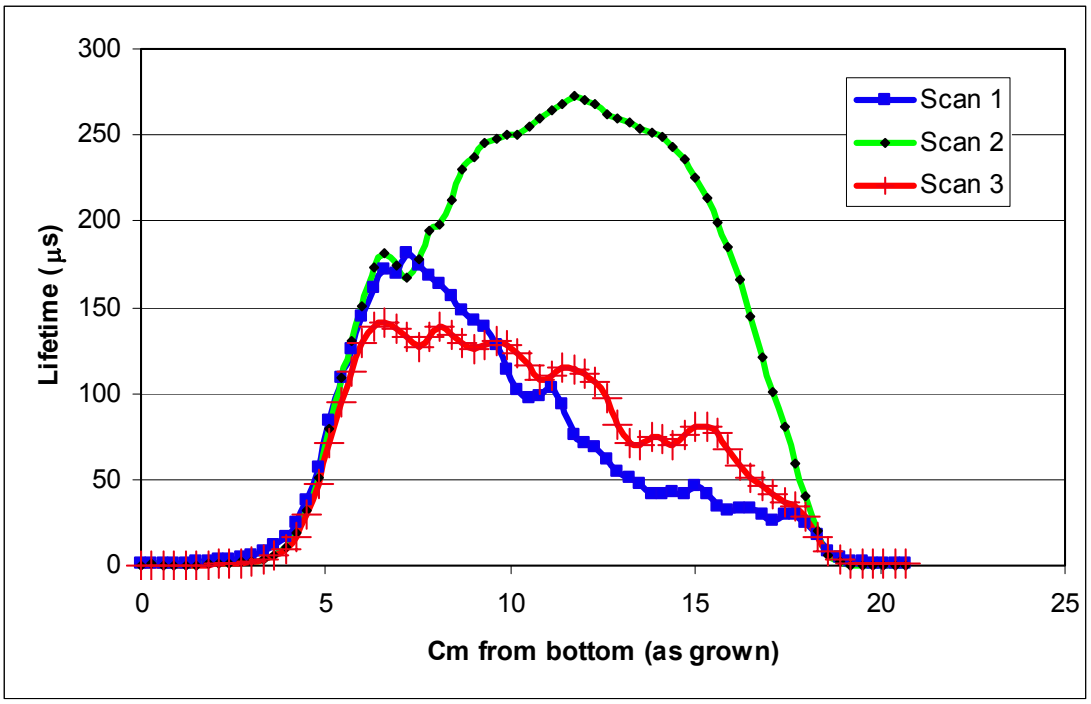

Fig. 30. Three linescans lengthwise up block C3-11523 after light-soaking

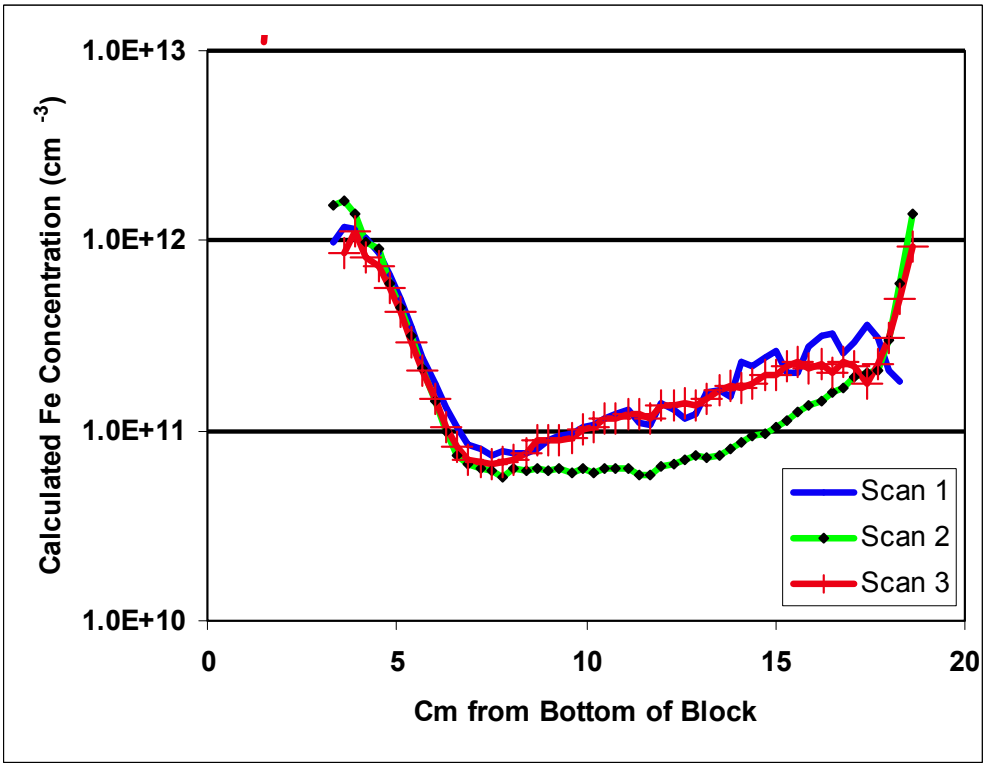

Fig. 31. For the regions with high lifetime, the data from the center block from the ingot, block C3-11523, was analyzed for iron concentration using the methodology of references (8) and (10).

The conversion of lifetime data to Fe concentration requires the minority-carrier density and resistivity of the material[10]. Both of these quantities were measured at each point in the block. The 850 nm IR-pass filter was used in this work because more photons are available than with the RG-1000 filter. This permitted the data to be taken at higher injection levels, nominally 7 x 10^{14} cm^{-3} in high-lifetime regions and 85% of the maximum achieved carrier density in the low-lifetime regions where 7 x 10^{14} cm^{-3} was not reached.

Figure 32 illustrates a practical application of the measurement of lifetime and Fe concentration data. Here, the components of the recombination rate are plotted vs. position in the block. When the recombination due to Fe is subtracted from the measured recombination, the result is predictive of the cell efficiency since typical cell processing will remove or passivate Fe[8]. Figure 32 indicates that if a decision is made to keep wafers that will have diffusion lengths greater than the cell thickness, 1 cm more silicon would be used from the bottom of the block, and 0.5 cm more from the top compared to the same decision not taking the effects of Fe into account. This extra 1.5 cm could represent 45 wafers.

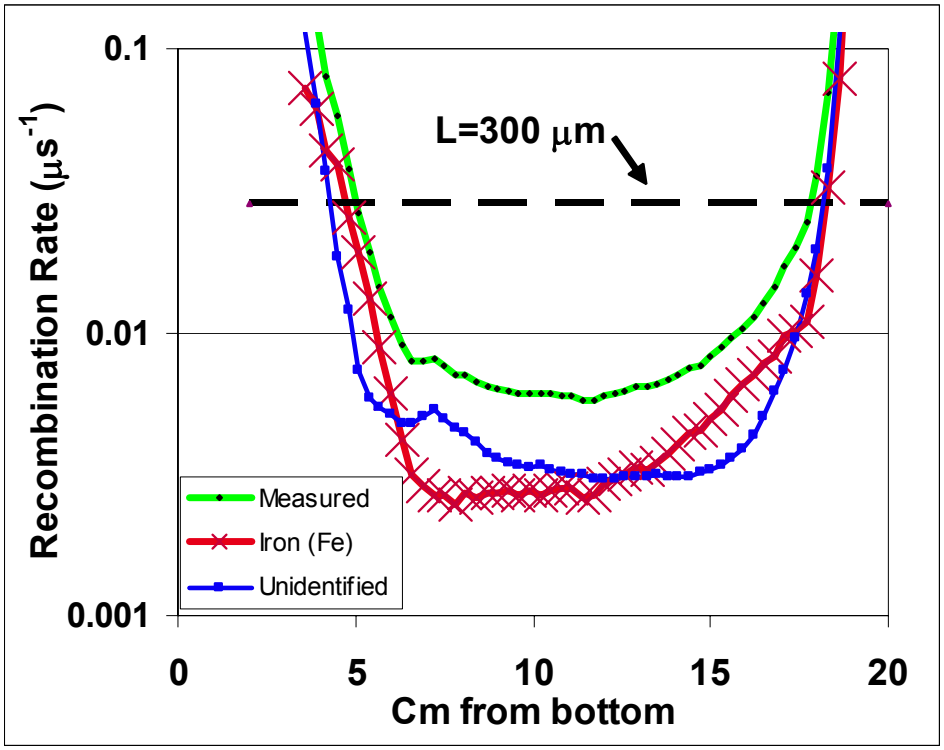

Fig. 32. The recombination due to iron calculated for the concentrations shown in Fig. 31. When this is subtracted from the measured data, the result, "unidentified" recombination, is predictive of cell performance[8]. The recombination rate where diffusion length equals cell thickness is shown for reference.

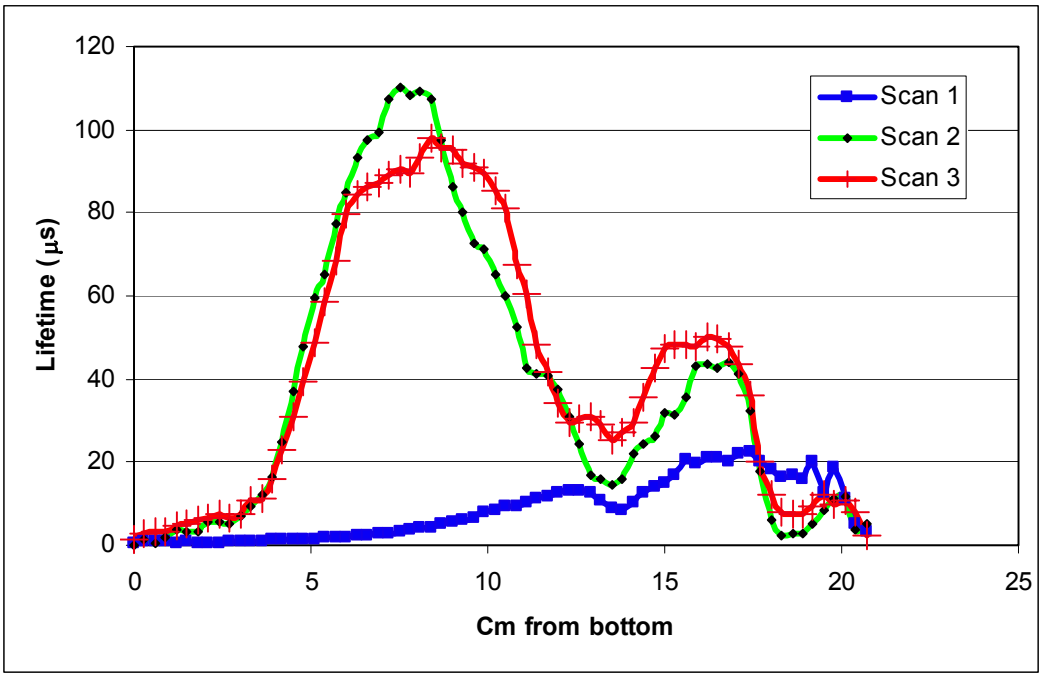

Fig. 33. The lifetime scans for a corner block from the ingot, E1-11523, with an interesting lower-lifetime feature at 13 cm.

Figure 33 shows lifetime scans from one face of a corner block from an ingot. This lifetime scan shows an interesting dip in lifetime, for all three scans, at about 13-14 cm. The calculated Fe concentration from this block, Fig. 10, does not show any peak in the Fe concentration at this point, indicating that dissolved Fe is not the cause of this low-lifetime region. Another parameter that was measured in these line scans was the "trapping" as defined in references [9] and [11]. This trapping has been shown to correlate with poor crystalline quality, including dislocation densities [8]. In Fig. 11, there is a strong peak in the trapping at the point where the lifetime dips.

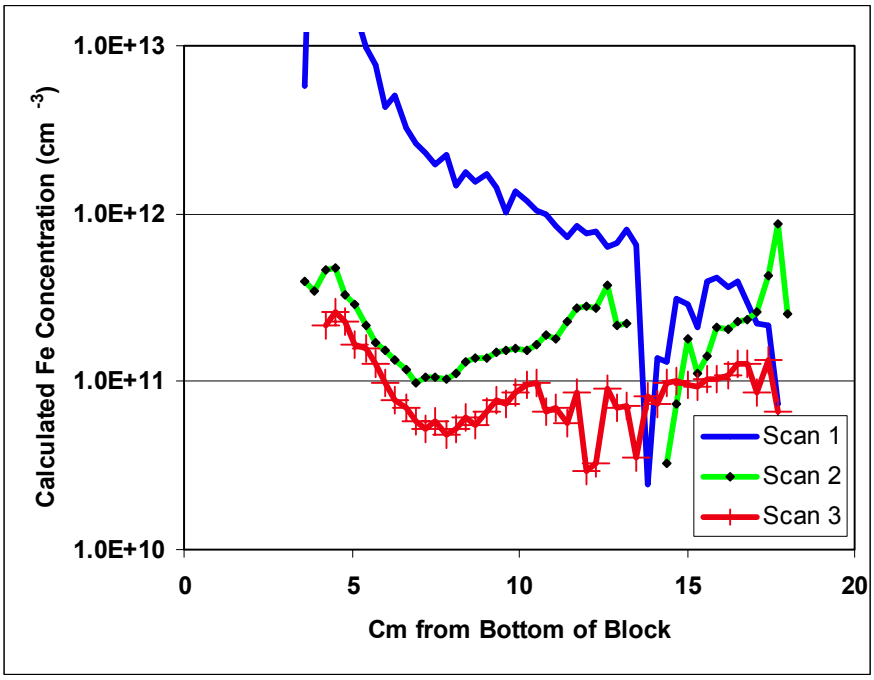

Fig. 34. The calculated Fe concentrations for the corner block shown in Fig. 33. The low-lifetime feature at 13 cm is apparently not correlated with high dissolved Fe concentration. In contrast, the low lifetime of one edge, labeled "scan 1" is directly correlated with the calculated Fe concentration.

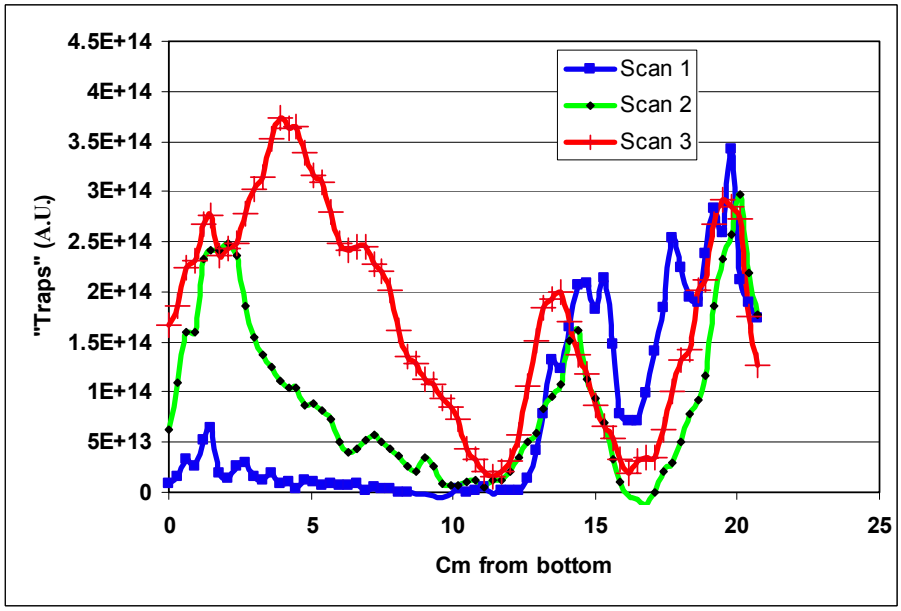

Fig. 35. Trapping, as defined in Ref [9] and [11] vs. position from the bottom of the block shown in Fig. 33 and Fig. 34. The strong dip in lifetime at 13-14 cm correlates with this trapping parameter.

Measurements such as those shown here, done on industrial blocks, have the potential to make a large impact on solar cell yields and efficiency. For example, it has been shown that the lower-lifetime regions at the top and the bottom of ingots respond dramatically differently to gettering processes, indicating that

there is a different optimal process for wafers with different defects[14]. If measurements at the block level could identify the different types of material, then they could be sorted so that the optimum process could be used for different "types" of wafer. This could give very significant improvements in efficiency and yield with little or no effect on costs. This strategy is illustrated in Fig. 36. For example, perhaps the silicon could be rated as being in 3 categories, as shown in this figure. The optimal process and cell design would be different for the 3 "wafer types" in order to obtain the maximum eventual module power from each type.

In an industry processing many hundreds of millions of multicrystalline wafers per year, any given line could be supplied with one of the types of wafers shown. The increased efficiencies, yields, and the better usage and recycling of silicon enabled by this kind of scheme could prove to be very significant for a reduction in cost per watt at the cell, module, and system levels.

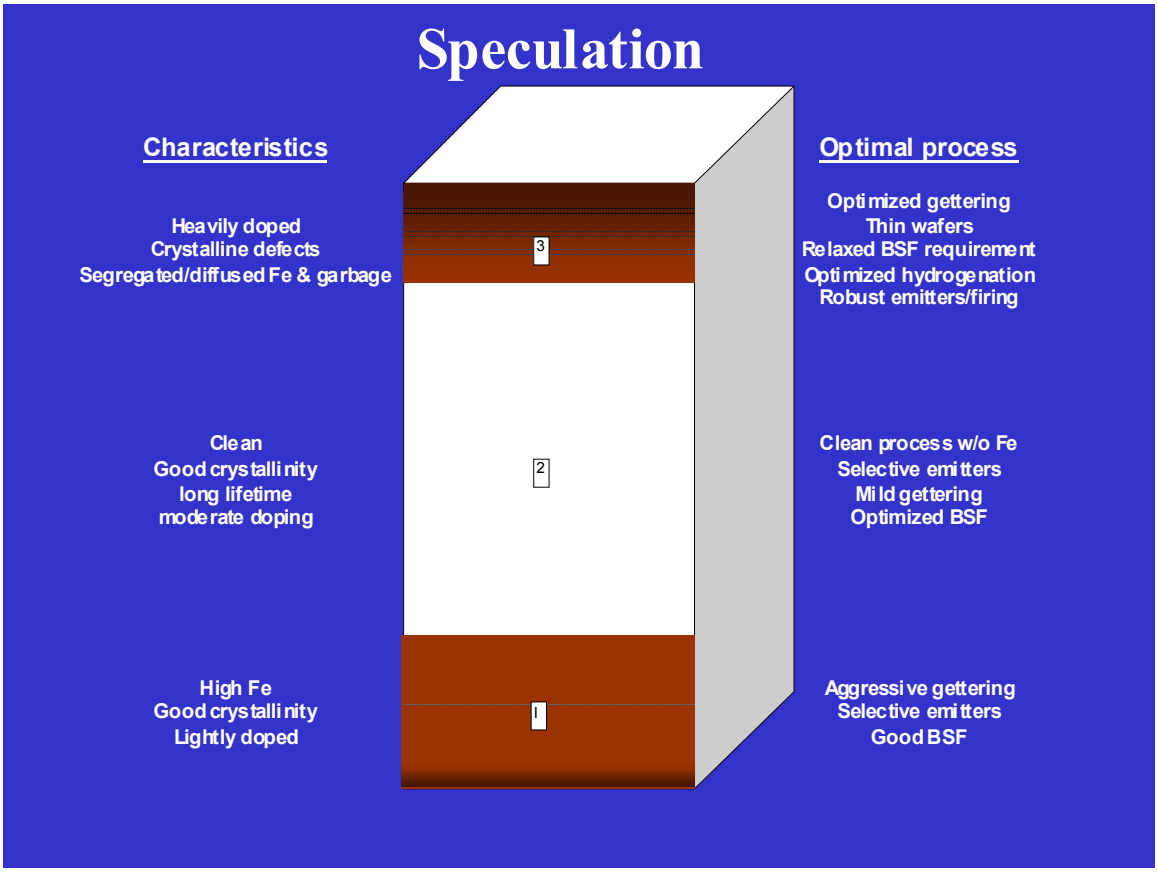

Fig. 36. A schematic indicating a provisional assignment of material type as a function of position in a multicrystalline brick of silicon. The material from each region would be more uniform than the spread of characteristics from the whole block. By running the material of each type through a different line, optimized for that particular silicon, yields and efficiencies could be significantly improved.

This would be in contrast to existing lines that have processes that have a process window wide enough to work moderately well for every wafer fabricated from a block. By definition, if different wafers respond to different processes, then a single process for all wafers results in lower than optimal efficiencies for most wafers. We look forward to the studies that would be necessary to prove out these possible gains.

Conclusions on Measuring Multicrystalline Blocks.

This application presented a methodology for obtaining calibrated quasi-steady-state photoconductance measurements on Si blocks. This was demonstrated by measuring lifetime, Fe, and trapping on multicrystalline blocks. The results show similar trends to previous studies done on wafers cut from various positions in silicon blocks and surface passivated with a nitride deposition[8]. In regions where Fe is known to diffuse into the crystal from the crucible or is frozen into the crystal at the top of the ingot, high-levels of Fe were observed resulting in low lifetime. Some other low-lifetime regions were present that did not correlate with dissolved Fe. In this initial study, these regions appear to correlate with trapping. The distinction is important, as poor lifetime due to Fe contamination can recover due to gettering and hydrogen passivation in the cell process. Poor lifetime due to poor crystalline quality is likely to result in solar cells with poor efficiency[8].

The results here support previous studies that indicate that better decisions can be made on which sections of a block to saw into wafers for processing and which sections to recycle [8]. This work demonstrates a method for obtaining this data on industrial blocks in the production process. This could provide immediate feedback to crystal growth in both research and industrial settings, as well as optimize the yields of wafered silicon into efficient solar cells.

Task 6. Develop 2nd-Generation, Commercial Sample-Head Instrument

There was a series of instruments that were developed under this project. By main application, these were:

-Boule tester (As shown in Fig. 4,5,13)

-Block scanner, (as shown in Fig. 7 and 9). The latest industrial version is shown in Fig. 37.

-In-line wafer-measurement tool. Many versions of this were developed including those shown in Fig. 14 and Fig. 20, and discussed in detail in those sections on the applications for measuring bare wafers.

All of these instruments were designed with aspects particular to the specific industrial application as envisioned.

However, each has the same central core sensor, and we have maintained a very general software that is capable of powering each application. The circuit boards went through several iterations to improve the functionality as required, as well as to integrate discrete components and simplify the fabrication of the instruments.

The block scanner and the 2-D data that results from scans required the development of new software for displaying the 2-D data. This software will soon be complete as the unit shown in Fig. 37 is fully characterized for the application on block scanning detailed under Task 5 in this report.

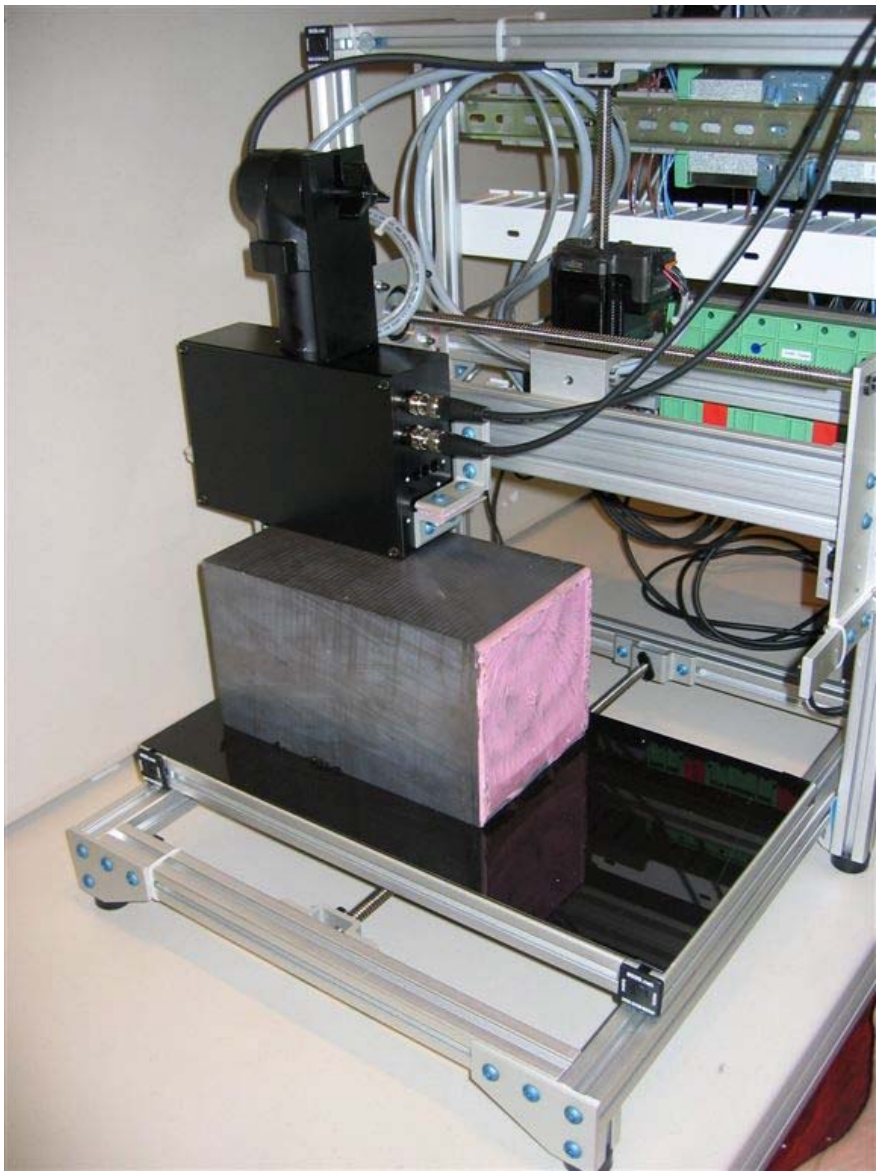

Fig. 37. The industrial version of the protype block tester with full automated 2-D scanning capability. This 2nd generation tool, compared to the instrument in Fig. 7, was developed during phase II of this subcontract.

In addition to the in-line lifetime measurement tasks in this subcontract, we also have developed an illumination vs. open-circuit voltage (Suns-V_{oc}) technique during this contract.

This Suns-V_{oc} technique has been generalized and improved during this contract. This technique, outlined in Ref. 16, measures the voltage as a function of illumination. This curve can then be translated by the short-circuit current, in order to display the data in the familiar form of an illuminated IV curve. This curve gives an upper bound on the efficiency that could be expected from the solar cell. This result is an upper bound because it is taken under open-circuit conditions, and therefore does not include any series resistance effects. In contrast, it includes shunt effects and all of the material properties that could lead to a soft fill factor. Comparison of this data with the final illuminated data from the solar cell can then definitively identify the series resistance losses[16].

This is especially useful for the development of the back-end process, where the firing temperatures and pastes must be optimized for the best compromise between shunting and series resistance.

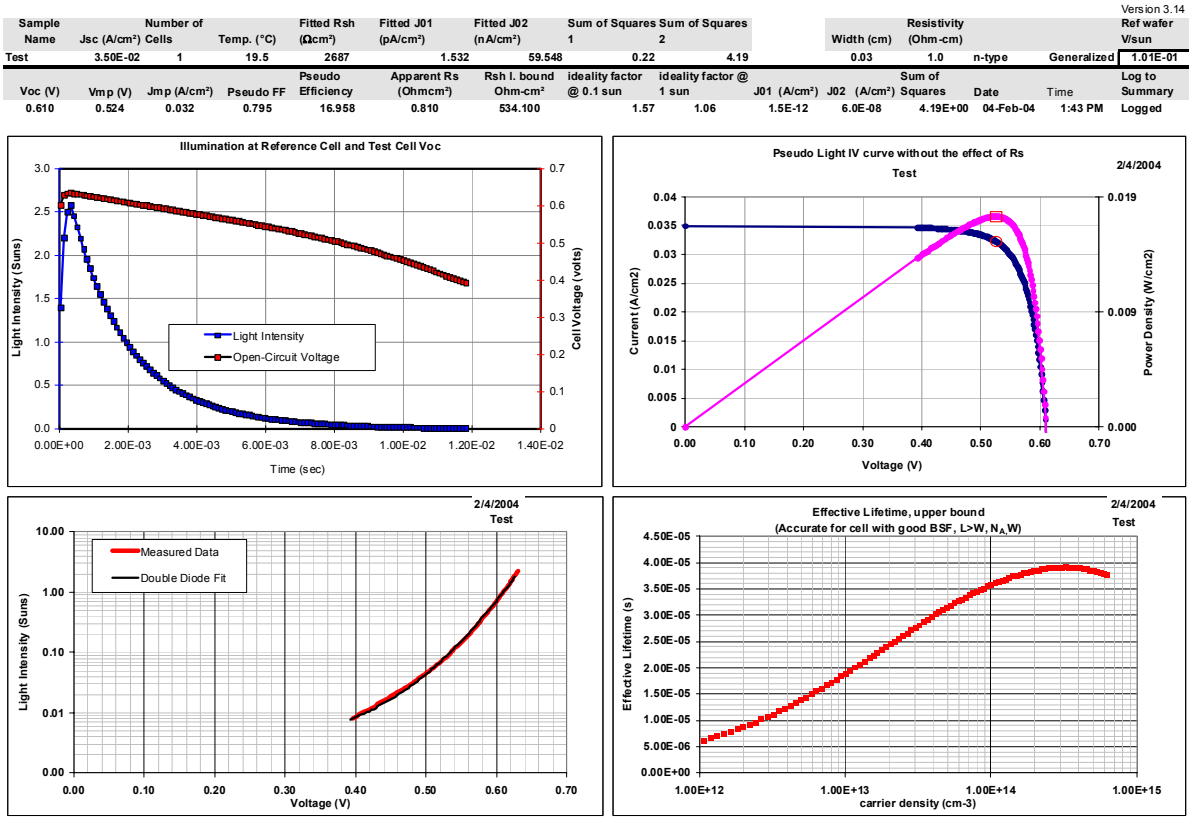

Fig. 38. Results from a detailed Suns-V_{oc} measurement

Several improvements were made to this measurement technique over the course of this subcontract. Fig. 38 shows the display from the standard Suns-V_{oc} program that runs off of the new 12-bit data acquisition system

The analysis improvements include:

1) The analysis was generalized from a pure steady-state analysis to one the uses the fully time-dependent equations. This allows for more accurate measurements of very-high-lifetime silicon solar cells, such as those by SunPower and Sanyo. Previously, there could be small errors for these high-lifetime (2 ms minority-carrier lifetime) solar cells when measured with the 2 ms decay rate in the flashlamp. This allows the IV curves to be constructed for any light pulse shape, ranging from a steady state condition all of the way to a transient condition, usually called open-circuit-voltage-decay, OCVD.
2) This improved accuracy enabled the conversion of this voltage data to lifetime data, as shown in the curve in the lower right-hand corner. This allows the direct comparison of lifetime and suns-V_{oc} data.
3) On the new data acquisition platform, all of these measurements can be made and logged to the database at a rate greater than 1 wafer per second.

Because the measurement is NOT contactless, the implementation into in-line applications in production lines has not gone forward yet. However, nearly every company ordering lifetime test equipment orders the Suns-Voc attachment as well, for process diagnostics. We have not pursued a probed implementation of this technology into the process line at this point in time. One place where this would happen in the fabrication process would be in processes where the Al BSF was fired prior to the front Ag screen print. A version of the Suns-V_{oc} system is shown in Fig. 39.

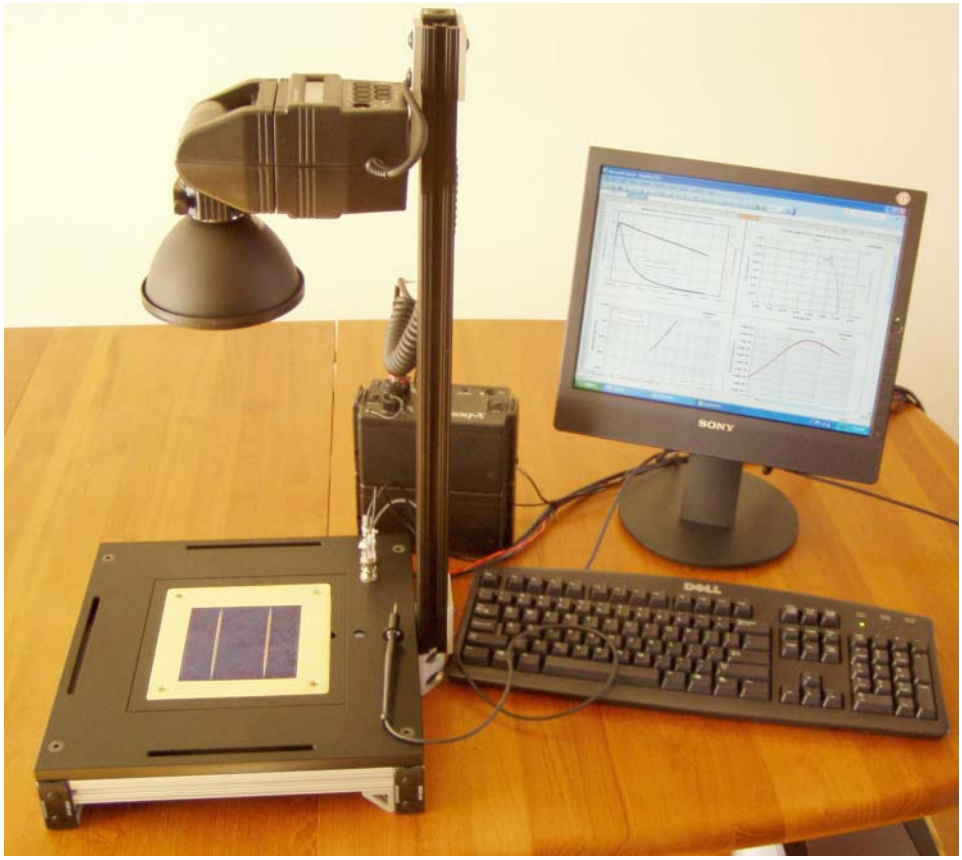

Fig. 39. The current version of the Suns-V_{oc} instrument. The large chuck can accommodate 6-inch wafers. The stage is magnetic, so that it can be used with magnetic-base probes.

It is more likely that Suns-V_{oc} will first appear in the production line at the stations where the cells are already probed. An example of this is shown in Fig. 40. This is a module measurement, with a single flash for the the Suns-V_{oc} curve, another flash to determine J_{sc}, and a third flash for the maximum power point. Based on this data, a full "IV curve without series resistance" can be constructed, and then the measured J_{sc}, V_{oc}, and load data points can be used to construct the full modeled IV curve.

This 3-flash protocol may be necessary to measure high-efficiency silicon solar cells. These cells have very high capacitance that slows the time response, prohibiting the type of voltage sweep during the flash that can be performed on lower-efficiency silicon cells [20].

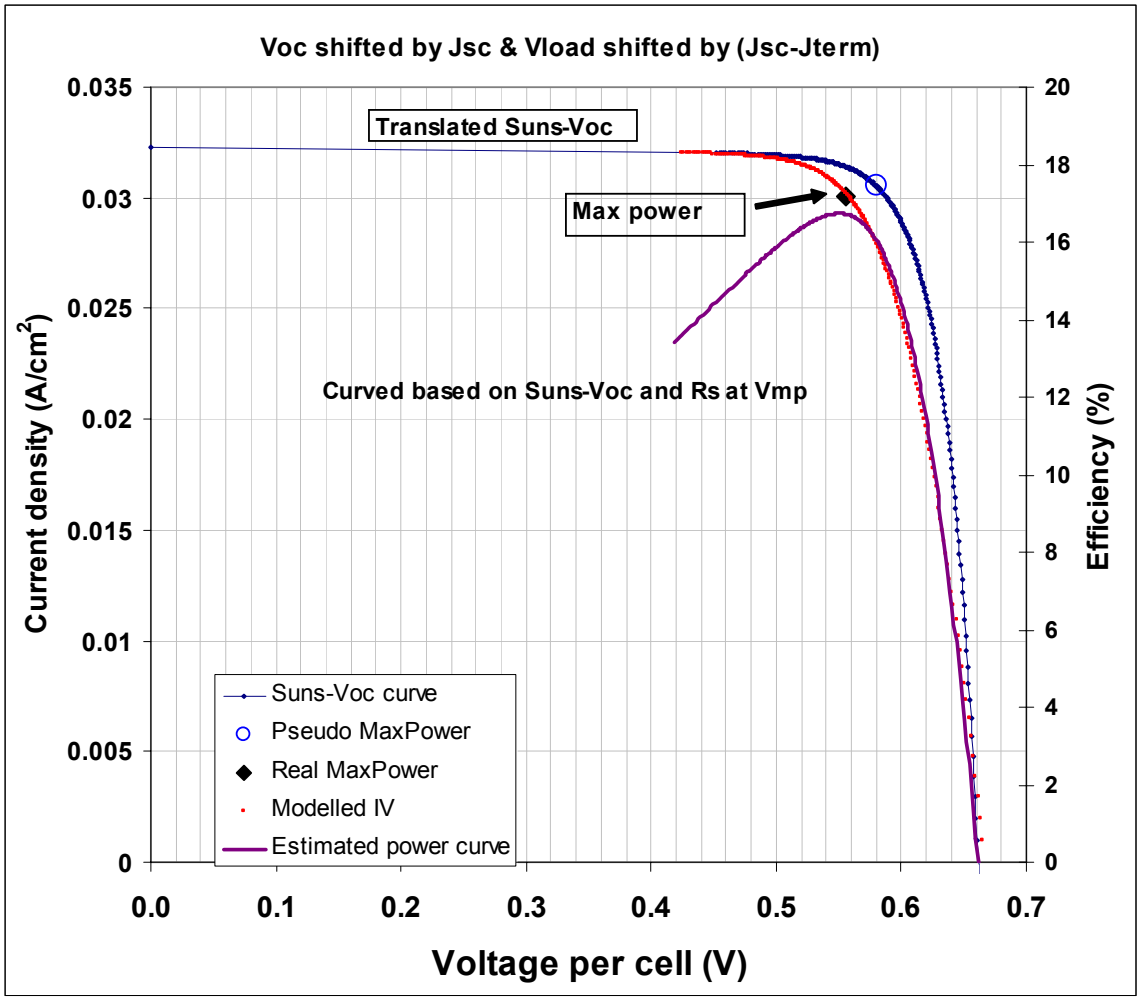

Fig. 40. A module measurement including a Suns-V_{oc} curve. The Suns-V_{oc} curve indicates the upper bound on the efficiency possible for the module. A comparison of this curve with the maximum power point indicates very precisely the losses due to series resistance in the module. Above, the maximum power point is measured during one flash pulse, the Suns-V_{oc} curve is measured during another and the short-circuit current is measured during the third. The power and IV curves are modeled based on this data. One point near V_{mp} can be determined for a high-efficiency solar cell in one pulse. The Suns-V_{oc} curve gives valuable process control information by allowing a clear identification of shunting and series resistance effects despite the difficulties in quickly obtaining the full illuminated IV curve for this type of solar cell or module made from these cells.

Contactless Spectral Response

Rather than developing the contact-less spectral response as a separate function[4], we have integrated the spectral response aspect as a critical component into all of our application notes. Several examples are given below, and have been discussed previously in this report.

In the bare wafer application note, light from the BG-38 visible-pass filter is used to measure the photoconductance of the bare wafer. The ratio of this response to that from the RG-1000 IR-pass filter can be used to determine the surface recombination velocity of the bare wafer. This value is then used to develop an accurate transfer function from measured to bulk lifetime for the wafer as a function of the wafer thickness, primarily using the data from the RG-1000 IR-pass filter.

In the application note on separating the bulk and surface recombination, the comparison of the lifetime measured with visible and IR light is shown to enable the separation of bulk and surface recombination effects, using an elaboration of the method proposed by Bail et al.[1].

The block and boule application also uses the BG-38 filter to discern whether the surface is passivated or not. For p-type CZ, we have found that it is not. Wafers show $S > 2x10^5$ cm/s. The transfer functions for measured to bulk lifetime are developed using PC1D simulations to allow us to report bulk lifetime based upon the measured lifetime. The same three filters were used in these studies, and built into the boule and multicrystalline block tester. The long-pass filter, the RG-1000 gives the measured lifetime requiring the least correction. However, it was found that for the application of determining the concentration of Fe as a function of position within silicon blocks, the RG-850 filter was preferred, since the intensity of light was much higher and a higher injection level could be achieved. This is important to reach the injection level that is preferred for the conversion of the lifetime data to Fe concentration.

Conclusions of this Final Subcontract Report

The objective of this subcontract over its two-phase, two year duration was to design and develop improvements to the existing Sinton Consulting R&D minority-carrier lifetime testers. The improvements would enable the possibilities for performing various in-line diagnostics on crystalline silicon wafers and cells for solar cell manufacturing lines in order to facilitate manufacturing optimization and process control.

The results of this subcontract are that four new instruments were developed and demonstrated. Each instrument focuses on a particular industrial application.

1) Inline minority-carrier lifetime and trapping measurement of wafers with a throughput rate of 1 per 2 seconds.
2) Measurement of minority-carrier lifetime in as-grown boules of CZ or FZ silicon.
3) Mapping of the lifetime, trapping, and Fe concentration in blocks of multicrystalline silicon.
4) The industrial use of illumination-Voc (Suns-V_{oc}) curves.

The development of these instruments involved a complete redesign of the basic common components of the tools, as well as the development of the features required for each application. Completely new data acquisition and user interfaces were developed. In order to adapt the measurement techniques to industrial samples, much of this work during this subcontract involved the development of application notes. These application notes are very forward looking in that they intended to make the latest R&D results directly applicable to industrial process control. In some cases, these application notes ran ahead of the state of the existing R&D in terms of device physics and analysis. We were able to present 12 R&D papers at technical conferences on this work and plan to present and publish several more. The R&D topics where we have been able to make contributions include:

-The generalization of Quasi-steady-state photoconductance lifetime measurements to silicon boules and blocks as they exist in industry (without any additional sample preparation).

-The use of spectral dependence of QSSPC to evaluate blocks and wafers.

-Mapping of lifetime, trapping, and Fe concentration using QSSPC on multicrystalline blocks.

-Interpretation of mapped lifetime data from blocks or wafers in order to predict solar cell efficiency.

-Obtaining an absolute calibration of lifetime and injection level for QSSPC and transient measurements on silicon blocks.

-The correlations between lifetime measured on CZ or multi-crystalline blocks of silicon and the resulting solar cell efficiencies.

Each of the tools that were developed benefited from industrial collaborators that contributed significant time and effort into joint experiments to define or evaluate each instrument. These collaborations were driven by our mutual interest in the potential usefulness of the resulting instruments and methods. As a result of these studies, we have published work jointly with authors from the solar cell manufacturing

industry. These publications will help with the industrial credibility by giving examples of results using precisely the conditions and sample types as they exist within industry. Several of these manufacturers have subsequently decided to implement these tools into their factories. A few "early adopters" already have the tools and have implemented testing on 100% of the silicon produced or used within the fabrication line. We are setting up for a commercial release of a line of new industrial instruments very soon.

References:

(work developed with support from this subcontract is marked with an *)

[1] Bail, M. and Brendel, R., 16th European Photovoltaic Solar Energy Conference, Glasgow, 2000, pp. 98-101.

[2] S. Bowden and R. A. Sinton, Proc. 14th NREL Silicon Workshop, Winter Park, CO 2004.

[3] P. A. Basore and D. A. Clugston, 26th PVSC Anaheim, 1977 pg. 207.

[4] T. F. Ciszek, T. H. Wang, M. Landry, A. Matthaus, G. B. Mihalik, Presented at the Electrochemical Society Joint Meeting, Oct. 1999.

[5] Thomas Clausen, Jan Vedde, Theis Leth Larsen, and Leif Jensen, and "Thin Monocrystalline Solar Cells Fabrication on Float Zone Silicon", Proc. PVSEC, Osaka, Japan, May 2003.

[6] *John L. Coleman, Jeff Nickerson, and Ronald A. Sinton, "Empirical Modeling of Ingot and Post Oxidation Level QSS Lifetime Measures in a Production Environment", NREL Workshop on Crystalline Si Materials and Processes, August, 2003.

[7] A. Cuevas and R. A. Sinton, "Characterization and diagnosis of silicon wafers and devices", Practical Handbook of Photovoltaics, T. Markvart and L. Castener Eds., Elsevier, Oxford. 2003.

[8] L. J. Geerligs, Proc. 3rd World Conference on PVSEC, Osaka, 2003.

[9] D. Macdonald and A. Cuevas, APL 74 (12) 22 March 1999, pp. 1710-1712.

[10] D. H. Macdonald, L. J. Geerligs and A. Azzizi, JAP 95(3) Feb.1 2004, pp.1021-1028.

[11] Daniel Macdonald, Ronald A. Sinton, and Andres Cuevas, "On the use of a bias-light correction for trapping effects in photoconductance-based lifetime measurements of silicon", J.A.P. Vol 89, (5) 1 March 2001.

[12] Keith R. MacIntosh, Michael J. Cudzinovic, David D. Smith, and William P. Mulligan and Richard Swanson, " The Choice of Silicon Wafer for the Production of Rear-Contact Solar Cells", Proc. PVSEC, Osaka, Japan, May 2003.

[13] Measurement by Daryl Myers, NREL, 2001.

[14] S. Riepe, M Ghosh, A. Muller, H. Lautenschlager, D. Grote, W. Warta, and R. Schindler, Proc. EPSEC, Paris 2004.

[15] Sinton, R.A. and Cuevas, A., Contactless determination of current-voltage characteristics and minority-carrier lifetimes in semiconductors from quasi-steady-state photoconductance data. Applied Physics Letters, 1996, 69(17), pp. 2510-2512.

[16] R. A. Sinton and A. Cuevas, in A Quasi-Steady-State Open-Circuit Voltage Method for Solar Cell Characterization, Proc. 16th European Photovoltaic Solar Energy Conference, Glasgow, Scotland, 2000.

[17] *Ronald A. Sinton, "Practical measurement of bulk lifetime and surface recombination by using wavelength dependence", Proc. PVSEC, Osaka, Japan, May 2003.

[18] *Ronald A. Sinton, "Predicting Multi-Crystalline Solar Cell Efficiency From Lifetime Measured During Cell Fabrication", Proc. PVSEC, Osaka, Japan, May 2003.

[19] * R. A. Sinton and T. Mankad, 13th NREL Workshop on Crystalline Materials and Processes, Aug. 2003.

[20] R. A. Sinton, "Testing High-Efficiency Solar Cells and Module", a draft white paper. WWW.sintonconsulting.com, April 2004.

[21] *R. A. Sinton, Tanaya Mankad, Stuart Bowden, and Nicolas Enjalbert, Proc. EPSEC, Paris 2004.

[22] *R. A. Sinton, Proc. 14th NREL Silicon Workshop, Winter Park, CO 2004 pp 152-157.

[23] *R. A. Sinton. NREL Annual Subcontract Report, /NREL/SR-520-35884 June 2003. Available at http://www.nrel.gov/docs/fy04osti/35884.pdf

[24] *Ronald A. Sinton, "Testing Solar Cell Wafers After Phosphorus Diffusion", Application note developed under DOE subcontract ZDO-2-30628-08. www.sintonconsulting.com, Unpublished.

[25] *R. A. Sinton, "Measuring and Monitoring Electronic Properties of Si During Industrial Material Preparation and Cell Fabrication, Proc. NREL PVAR&D meeting", March, 2003.

[26] *Ronald A. Sinton , "Boule Test Application Note", Application note developed under DOE subcontract ZDO-2-30628-08. Sintonconsulting.com, Unpublished.

[27] *Ronald A. Sinton, "Testing Bare Wafers using the Sinton Consulting WCT-100 Lifetime Tester", Application note developed under DOE subcontract ZDO-2-30628-08. Sintonconsulting.com, Unpublished.

[28] R. A. Sinton, Harsharn Tathgar, Stuart Bowden, and Andres Cuevas, **"**On the problem of determining the bulk lifetime of unpassivated silicon wafers**"** 14th NREL Silicon Workshop, Winter Park, CO 2004.

[29] Jan Vedde, Leif Jensen, and Thomas Clausen, "Float zone silicon for High Volume Production of Solar Cells", Proc. PVSEC, Osaka, Japan, May 2003.

REPORT DOCUMENTATION PAGE

Form Approved
OMB No. 0704-0188

PLEASE DO NOT RETURN YOUR FORM TO THE ABOVE ORGANIZATION.

1. REPORT DATE *(DD-MM-YYYY)*	2. REPORT TYPE	3. DATES COVERED *(From - To)*
December 2004	Subcontractor Report	2 August 2002–15 November 2004

4. TITLE AND SUBTITLE
Development of an In-line Minority-Carrier Lifetime Monitoring Tool for Process Control during Fabrication of Crystalline Silicon Solar Cells: Final Technical Report, 2 August 2002–15 November 2004

5a. CONTRACT NUMBER
DE-AC36-99-GO10337

5b. GRANT NUMBER

5c. PROGRAM ELEMENT NUMBER

6. AUTHOR(S)
R.A. Sinton

5d. PROJECT NUMBER
NREL/SR-520-37212

5e. TASK NUMBER
PVB56101

5f. WORK UNIT NUMBER

7. PERFORMING ORGANIZATION NAME(S) AND ADDRESS(ES)
Sinton Consulting, Inc.
1132 Green Circle
Boulder, Colorado 80305

8. PERFORMING ORGANIZATION REPORT NUMBER
ZDO-2-30628-08

9. SPONSORING/MONITORING AGENCY NAME(S) AND ADDRESS(ES)
National Renewable Energy Laboratory
1617 Cole Blvd.
Golden, CO 80401-3393

10. SPONSOR/MONITOR'S ACRONYM(S)
NREL

11. SPONSORING/MONITORING AGENCY REPORT NUMBER
NREL/SR-520-37212

12. DISTRIBUTION AVAILABILITY STATEMENT
National Technical Information Service
U.S. Department of Commerce
5285 Port Royal Road
Springfield, VA 22161

13. SUPPLEMENTARY NOTES
NREL Technical Monitors: D. Mooney and K. Brown

14. ABSTRACT *(Maximum 200 Words)*

The objective of this subcontract over its two-phase, two-year duration was to design and develop improvements to the existing Sinton Consulting R&D minority-carrier lifetime testers. The improvements enable the possibilities for performing various in-line diagnostics on crystalline silicon wafers and cells for solar cell manufacturing lines. This facilitates manufacturing optimization and improved process control. The scope of work for Phase I was to prototype industrial applications for the improved instruments. A small-sample-head version of the instrument was designed and developed in this effort. This new instrument was complemented by detailed application notes detailing the productive use of minority-carrier lifetime measurements for process optimization and routine process control. In Phase II, the results from the first year were applied to design new instruments for industrial applications. These instruments were then characterized and documented. We report here on four new instruments, each optimized for a specific application as demanded by industrial customers. The documentation for these instruments was very technical and involved considerable R&D. Applications were developed that applied the latest in R&D on industrial silicon materials. By investigating the compromises that would be necessary to measure industrial material directly without the sample preparation that is commonly done for good research, we were able to develop several very innovative applications that can now be done directly in the production line for process control.

15. SUBJECT TERMS
PV; module; solar cells; manufacturer; minority-carrier lifetime; crystalline silicon wafers; breadboard components; lifetime monitoring tool; in-line measurements; photoconductance; phosphorus diffusion; short-circuit current;

16. SECURITY CLASSIFICATION OF:			17. LIMITATION OF ABSTRACT	18. NUMBER OF PAGES	19a. NAME OF RESPONSIBLE PERSON
a. REPORT	b. ABSTRACT	c. THIS PAGE			19b. TELEPONE NUMBER (*Include area code)*
Unclassified	Unclassified	Unclassified	UL		